Optimizing Borehole Heat Exchanger Spacing to Maximize Advective Heat Transfer

A THESIS
SUBMITTED TO THE FACULTY OF
UNIVERSITY OF MINNESOTA
BY

Jennifer Meester

IN PARTIAL FULFILLMENT OF THE REQUIREMENTS
FOR THE DEGREE OF
MASTER OF SCIENCE

Advisor: Martin Saar, PhD

September 2013

Table of Contents

Abstract

This generalized study provides first order insights into the effect of heat advection on ground source heat pump (GSHP) system operation and the optimization of spacing between borehole heat exchangers (BHE) using groundwater flow and heat transport models. In these systems, there is a threshold Péclet number, the ratio of heat advection rate to heat conduction rate, beyond which the efficiency of heat transfer between the BHEs and the aquifer is significantly increased, thus lowering the temperature drop of the circulating fluid in the BHE and increasing the overall efficiency of the BHE system. This threshold Péclet number depends on the groundwater flow rate and effective thermal diffusivity (among other factors) of the system and, for the given conditions, is approximately 2 with a 1% change in BHE outlet temperature and approximately 11 with a 5% change. In GSHP systems with standardized spacings between BHEs, groundwater heat advection can cause negative thermal interactions between heat exchangers, which can be eliminated and in some situations replaced with positive thermal interactions by optimizing the spacing between BHEs. Above the threshold Péclet number, there is specified spacing between heat exchangers that will allow for the utilization of the previous season's heat injection or extraction, a half year transport distance. For the GSHP system simulated in this study, the BHE spacings for optimization are 6.65 m and 13.8 at groundwater flow velocities of 2.5×10^{-5} m/s and 5×10^{-5} m/s, respectively. It may also be possible to space the heat exchangers at a distance that captures heat after a year and a half of transport (for systems with only slight heat advection dominance), but more simulations are necessary to investigate the results of such a strategy.

List of Tables

List of Figures

1. Introduction

In this study, I investigate the impact of heat advection on GSHP operation to provide first order insights and optimize the spacing between heat exchangers to utilize the positive impacts of heat advection by using computer models for groundwater flow and heat transport. The impact of groundwater heat advection is analyzed for a GSHP system with no thermal interaction between BHEs for various operational durations and effective thermal diffusivities during the course of one summer cooling season. The same analysis is performed for a GSHP system with thermal interaction between BHEs. The effects of thermal interference on system performance efficiency are also analyzed for the simulations with multiple heat exchangers. The optimal spacing between BHEs for the utilization of the heat injected/extracted in the previous season is determined for the GSHP system and is then applied in multi-season simulations with both summer cooling and winter heating seasons. Finally, the long term impact of heat advection on GSHP operation is evaluated using ten-year-multi-season simulations for a system with no thermal interactions between BHEs.

The majority of previous studies have focused on simulating the conductive heat exchange within and surrounding a single borehole heat exchanger (BHE). These methods provide reasonable estimates of heat exchange and temperature fields when groundwater flow and thermal interactions between BHEs do not occur, but this is rarely the case in practical applications. When groundwater flow does occur in the ground

source heat pump (GSHP) field, the heat exchange that occurs between the borehole heat exchanger and its surroundings may be significantly underestimated by simulations that only account for conductive heat transfer. This is because the process of groundwater flow advects heat from (during subsurface heat injection) and to (during subsurface heat extraction) the BHE and therefore increases heat exchange between the BHE and the aquifer (Fan et al., 2007).

Some previous studies have included advective heat transport into their modeling approach. They found that including groundwater flow in ground source heat pump systems significantly impacts the performance of borehole heat exchangers (Sutton et al., 2003; Fan et al., 2007), affects the temperature distribution in the aquifer surrounding the BHE (Sutton et al., 2003), and influences thermal response tests (Raymond et al., 2011). These effects of groundwater flow occur when the groundwater velocities exceed a specific threshold for a given GSHP system, and below that threshold there are minimal to no advective heat transport effects. Therefore, the combined processes of heat conduction, heat advection, and mechanical thermal dispersion should be considered when simulating heat transport in areas with significant groundwater flow where heat advection is dominant (Péclet numbers greater than one).

Heat advection by groundwater can affect the performance of ground source heat pump systems positively or negatively. However, there have been few studies that optimize the design of GSHP systems in order to maximize the positive impacts of heat advection.

Through proper spacing of heat exchangers in dual season GSHP systems, it should be possible to capture excess heat injected into the aquifer, during summer cooling operations, for heating in the following season (or to transport heat away from the BHE for use in cooling when the seasons are reversed). There have been some studies into dual season GSHP systems (e.g., Fan et al., 2007; Michopoulos and Kyriakis, 2009), but these studies have not focused on optimizing the positive thermal interference between BHEs to utilize energy stored seasonally within the aquifer.

Methods

1.1. Conceptual model used in simulations

The conceptual model (Figure 1) consists of 200 rows and 500 columns at a regular grid spacing of 0.1m and a single, horizontal 100m-thick layer. A previous study by Lee (2011) found that such a single-layer model can be appropriately used to model ground source heat pump systems with multiple ground layers that have varying permeabilities and/or porosities and different thermal diffusivities. Such single layer models have since been employed in the simulation of borehole heat exchangers by Koohi-Fayen and Rosen (2012) and Florides et al. (2012).

To simulate the flow field, initial hydraulic heads (referred to hereafter as "heads") are assigned to each cell at the beginning of the simulation. The head gradient is calculated based on Darcy's Law (Darcy, 1856; Bobeck, 2004) for fluid flow through a porous medium at specified groundwater flow velocities. The flow domain boundary conditions are set as no-flow boundary conditions at the top and bottom outer edges of the domain and constant-head boundary conditions at the left and right outer edges of the domain.

To simulate the temperature field, a uniform initial temperature approximately equal to the undisturbed temperature of the ground in Minnesota, 12 °C, is assigned to each cell in the model domain. The undisturbed temperature of the ground is close to the mean annual

surface temperature below a minimum depth of about 2 meters, with the ground effectively serving as a low-pass filter of seasonal temperature variations. The temperature domain boundary conditions are set as no-thermal-flux boundary conditions at the top and bottom outer edges of the domain and constant-temperature conditions, equal to the initial temperature, applied at the left and right outer edges of the horizontal domain.

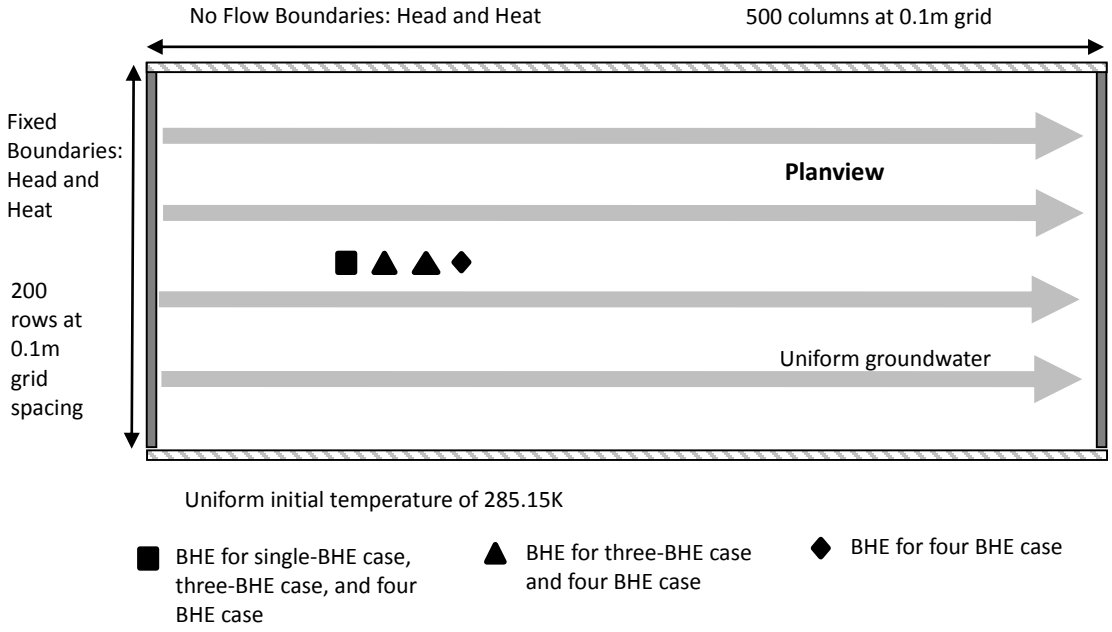

Figure 1: Conceptual model in map view for the single-BHE case, the three-BHE case, and the four-BHE case. The model domain is a single 100m-thick, horizontal layer. The single-BHE case simulates no thermal interference systems and is used in determining the optimal BHE spacing; the three-BHE case simulates thermal interference systems; and the four-BHE case simulates optimized BHE fields.

For the simulations without interference between heat exchangers, a single BHE fully penetrating the aquifer was placed within the model domain (at row 100, column 100), as shown in Figure 1. A constant heat transfer of 25 W/m into the aquifer for summer cooling was applied at the BHE. A constant heat flux at the BHE can be justified when the thermal distribution throughout the aquifer including thermal interference between BHEs is of more concern than the dynamic heat exchange within the borehole occurring between the borehole wall, grout, piping and circulating fluid (Koohi-Fayeh and Rosen, 2012). In this case, the temperature distribution within the borehole will have minimal impact on the temperature distribution of the surrounding aquifer.

The specific installed thermal output/input for a ground source heat pump system determines the heating capacity of each borehole per meter length (Banks, 2008). BHEs operate at various heat exchange rates. Thus, previous studies have used a wide range of heating powers to simulate GSHP systems: Choi et al. (2013) used a heat exchange rate of 10 W/m, Koohi-Fayeh and Rosen (2012) used rates of 5, 10, 15, and 50 W/m^2, Raymond et al. (2011) used a rate of 32.8 W/m, Hecht-Méndez et al. (2010) used a rate of 60 W/m, and Mottaghy and Dijkshoorn (2012) used rates varying between 20.8 and 207 W/m. Given this wide range (5-207 W/m) of heat exchange rates previously used in simulations, 25 W/m and 10 W/m (discussed later) are applied to the BHE. These values are well within the range of heat exchange rates typically used in industry and previous simulations of borehole fields and are representative of rates used in practical heating and cooling applications.

For simulations with interference between heat exchangers, three BHEs that fully penetrate the aquifer were placed within the model domain parallel to the groundwater flow direction, as shown in Figure 1. Three heat exchangers are used so that the center BHE may potentially be impacted by both heat conduction from the two adjacent BHEs and heat advection from the upstream BHE. The spacing between BHEs is 5m for the interference simulations, which is based on the spacing between BHEs recommended by Chiasson et al. (2000) and Banks (2008) and the spacing used in previous studies (Koohi-Fayeh and Rosen, 2012; Choi et al., 2013). A constant heat exchange of 25 W/m was applied at the BHEs for the duration of a summer cooling season as described above.

To simulate optimized BHE fields, four fully penetrating BHEs (instead of the three used previously) were placed within the model domain parallel to the groundwater flow direction, as shown in Figure 1. For these simulations, three different groundwater flow velocities are used: 5×10^{-5} m/s, 2.5×10^{-5} m/s, and 1×10^{-5} m/s. As shown later, for the given conditions (e.g., porosity, thermal diffusivity), the BHE spacing for optimization is 13.8 m at a groundwater flow velocity of 5×10^{-5} m/s, 6.65 m at a groundwater flow velocity of 2.5×10^{-5} m/s, and 2.5 m at a groundwater flow velocity of 1×10^{-5} m/s. Four 90-day seasons (simplifying the year to 360 days) are simulated for each of two years: a summer cooling season with a constant heat injection rate into the ground of 10 W/m, a fall season of no BHE operation, a winter heating season with a constant heat extraction rate out of the ground of 10 W/m and a spring season of no BHE operation. A lower heat exchange rate is used for these simulations (10 W/m instead of 25 W/m) as 90 days of

continuous heat extraction causes freezing of the ground and the circulating fluid within the BHE for the given conditions at the higher heat extraction rate.

For ten-year simulations with a single heat exchanger, the fully penetrating BHE was placed within the model domain, as shown in Figure 1. For these simulations, three different groundwater flow velocities are used: 5×10^{-5} m/s, 2.5×10^{-5} m/s, and a no-groundwater-flow case (0 m/s) with a 10 W/m heat exchange rate and the same seasonal heating pattern described above.

1.2. Computer models for groundwater flow and heat transport

In this study, computer models are used to simulate the heat transfer from the borehole heat exchangers to the region outside the boreholes. MODFLOW-2005 (Harbaugh, et al. 2000; Harbaugh, 2005) simulates the groundwater flow of the GSHP system and is coupled either with MT3DMS (Zheng and Wang, 1999; Zheng et al., 2001; Zheng, 2009; Zheng, 2010) or with SEAWAT (Guo and Langevin, 2002; Langevin et al., 2008) to simulate heat transport within the aquifer. MODFLOW-2005 is a modular groundwater flow simulator that employs a block-centered finite difference approach. MT3DMS, or Modular 3-D Transport Model Multi-Species, and SEAWAT simulate heat transport within a porous medium by treating heat as a "solute" species. Since the equations for solute transport and heat transport are mathematically analogous, MT3DMS and SEAWAT, though designed for solute transport, are also applicable to heat transport.

The simulations that follow use MT3DMS which is one-way coupled with MODFLOW-2005, the groundwater flow simulator. Changes in groundwater temperature caused by solution of the heat advection diffusion equation are assumed to cause only negligible variations in water density and therefore have no significant impact on the groundwater flow field, which holds true for small differences in temperature. However, feedback between the groundwater flow and heat transport models may theoretically be needed as changes in temperature affect hydraulic conductivity by changing certain water properties, namely density and dynamic viscosity, and can thus cause buoyancy-driven

convection. In cases where significant changes in water density do occur, the groundwater flow and heat transport simulations must be coupled to allow feedback between solutions (Zheng and Bennet, 2002). In the shallow subsurface, where ground source heat pump systems are used, the temperature changes are normally small enough that errors caused by assuming a constant hydraulic conductivity are negligible (Hecht-Méndez et al., 2010).

Prior to deciding to solely use MT3DMS, the performance of MT3DMS and SEAWAT in simulating the heat exchange from a single BHE into an aquifer and the resultant temperature distribution were compared. SEAWAT, unlike MT3DMS, allows for feedback between the groundwater flow and heat transport models and is thus two-way coupled with MODFLOW. The two models were found to produce results with no significant difference (for an example see Appendix A) as the temperature variations in the systems modeled were relatively small, and therefore did not have a significant impact on the groundwater flow field.

1.3. Heat transfer inside the borehole

Modeling of GSHP systems is typically approached by splitting the systems into two regions: the region inside the borehole and the region surrounding the borehole.

For long-term analyses of GSHP system behavior, the temperature of the borehole wall can be determined based on the simulation of the temperature field of the surrounding aquifer. Then the borehole wall temperature along with the characteristics of the BHE can be used to calculate the circulating fluid temperature at the inlet and outlet of the BHE. This method of coupling the regions inside and outside the borehole by treating the BHE as a constant heat source/sink and modeling the heat exchange within the aquifer, assumes the heat transfer processes between the heat exchanger and the surrounding media is instantaneous.

1.3.1. Simulating the BHE as a constant energy source/sink

Within the simulators, there are two main methods to specify the heat exchange between the BHE and the surrounding aquifer. The BHE can either be assumed to be at a constant (or temporally varying) temperature (i.e., a potential condition) or to have a constant (or temporally varying) heat energy flux (i.e., a flux condition). In the constant temperature BHE scenario, the circulating fluid and the borehole are assumed to remain at a constant average temperature. The amount of heat injected (or extracted) into the aquifer varies as the temperature of the region surrounding the aquifer varies. In the constant heat energy flux scenario, the amount of heat injected (or extracted) into the aquifer is assumed to be constant. The average borehole wall temperature and the outlet temperature of the BHE vary with the temperature of the surrounding region to allow for the specified heat energy flux. Both methods were explored, and the constant energy flux condition was chosen to represent the BHE, as the specific installed thermal output/input for a ground source heat pump system determines the desired heat exchange rate of each borehole per meter length (Banks, 2008). Thus, the heat exchange rate between each BHE and the aquifer is specified, and the temperature of the circulating fluid in the heat exchanger varies to meet the heating/cooling needs of the system.

In this study, a specified amount of energy is injected (or extracted) at the BHE into (or out of) the ground. In MT3DMS and SEAWAT, this is best achieved by designating the BHE as a mass-loading source and assigning a temperature-loading rate directly to the

BHE. Typically, these models are used for solute transport simulations and therefore the mass-loading source must be adapted for use as a temperature-loading source. The mass-loading rate is related to the heat-loading rate through the following equation (Hecht-Méndez et al., 2010):

$$q_{ss}C_{ss} = \frac{q_h}{\rho_w c_{pw}} \qquad (1)$$

where q_{ss} is the flow rate taken from the flow model (in this case MODFLOW), C_{ss} is the solute source concentration, and q_h is the volumetric heat input/extraction.

For a mass-loading source, the solute source concentration is assigned directly as the mass-loading rate (the left side of Equation 4) of the source with no flow rate needed from the model. Thus, for a heat-loading source with a constant energy flux, the heat-loading rate (the right side of Equation 4) of the source is assigned directly to the source cell. This rate can be calculated from the constant heat input/extraction rate specified for the BHE.

1.4. Heat transfer outside the borehole

The simplest models used to estimate the heat transfer from BHEs without explicitly modeling the region inside the borehole are the infinite line source model (Ingersoll, 1954) and the infinite cylindrical source model (Carslaw and Jaeger, 1959). These two approaches model one-dimensional conduction perpendicular to the borehole axis in an infinite, isotropic, and homogenous porous medium, assuming an infinite source with a constant heat flux per unit length, radial and purely conductive heat transfer from the source, uniform initial temperature and a constant temperature at an infinite radial distance from the source. A two-dimensional analytical solution adapted from Carslaw and Jaeger (1959) and Taler and Duda (2006) is used in this study as a preliminary validation of MT3DMS and SEAWAT for modeling a BHE with purely conductive heat transfer (see Appendix A). These models do not consider the impact of heat advection, which may be significant in regions with appreciable groundwater flow, as is the premise of this study.

There are also some analytical solutions that include simple configurations of advective heat transfer in two-dimensions that have been applied to borehole heat exchangers. Metzger et al. (2004) modeled the temperature response of an infinite and constant line source in an infinite, isotropic, and homogeneous porous medium under transient conditions with groundwater flow velocities considering heat dispersivities. Diao et al. (2004) also modeled the temperature response of an infinite and constant line source in an

infinite, isotropic, and homogeneous porous medium with groundwater flows, but under steady-state conditions and without considering heat dispersivity. Hecht-Méndez et al. (2010) modified this equation to include heat dispersivity. While these analytic solutions consider the impact of heat advection, they do not account for multiple heat exchangers or the thermal interactions that may occur between them. Also, given the assumptions that have been applied to derive the solutions, numerical models account for greater variability (e.g., anisotropic and heterogeneous porous mediums and variations in the temperature field) within the real-world ground source heat pump systems. For this reason, computer models were used to simulate groundwater flow (MODFLOW) and both conductive, advective, and dispersive heat transport (MT3DMS).

Heat conduction is a slow process driven by the temperature gradient and is described by Fourier's law (Fourier, 1822; Saar, 2011) as follows:

$$\mathbf{q_{h_c}} = -\mathbf{K_T} \cdot \nabla T$$

where $\mathbf{q_{hc}}$ is the conductive heat flux for a unit cross-sectional area, $\mathbf{K_T}$ is the thermal conductivity, and T is the temperature. The heat conduction equation analogous to the groundwater flow equation is the thermal-diffusion equation (Saar, 2011) as follows:

$$\frac{\partial T}{\partial t} = \nabla \cdot \left(\frac{\mathbf{K_T}}{\rho c} \cdot \nabla T\right) + S_h$$

where ρc is the effective volumetric heat capacity of the porous media and S_h represents the heat sinks or sources.

Comparatively, heat advection is a relatively fast process compared to heat conduction and is driven by groundwater flow as the fluid transports heat. The heat advection diffusion equation (Saar, 2011) describes heat advection:

$$\frac{\partial T}{\partial t} = -\frac{\rho_w c_w}{\rho_{eff} c_{eff}} \nabla \cdot (\mathbf{q}T) + \mathbf{D}_{\mathbf{T_{eff}}} \nabla^2 T$$

where $\rho_w c_w$ is the volumetric heat capacity of water, $\rho_{eff} c_{eff}$ is the effective volumetric heat capacity of the porous media, and $\mathbf{D}_{\mathbf{Teff}}$ is the effective thermal diffusivity. The heat advection-diffusion equation is the governing equation used in this study describing both heat advection and heat conduction processes.

1.5. Physical properties of the numerical model

The physical properties of the aquifer and borehole used in the simulations are summarized in Table 1. The physical properties are chosen based on those for a sandy aquifer. The transmissivity, $T=Kb$, is chosen based on the hydraulic conductivity, K, values for a sandy aquifer from Freeze and Cherry (1979) and the 100-m thickness, b, of the model aquifer. Typical values for sandy aquifers are chosen for the confined storage coefficient, porosity, and dispersivities of the aquifer. Here, the confined storage coefficient is the volume of water released from a confined aquifer per unit change in hydraulic head per unit surface area (U.S. Department of the Interior, 1955). The thermal conductivity, density and specific heat capacity of the sand were chosen based on the thermal conductivity and diffusivity experiments of Nakshabandi and Kohnke (1965).

The effective thermal conductivity was calculated based on the values from Nakshabandi and Kohnke (1965) using the following equation:

$$k_{eff} = n \times k_w + (1 - n) \times k_s \qquad (2)$$

where k_{eff} is the effective thermal conductivity, n is the porosity, k_w is the thermal conductivity of water, and k_s is the thermal conductivity of sand.

The effective thermal diffusivity was calculated using the same values and the following equation:

$$\alpha = \frac{k_{eff}}{n \times \rho_w \times c_{pw} + (1-n) \times \rho_s \times c_{ps}} \qquad (3)$$

where α is the effective thermal diffusivity, k_{eff} is the effective thermal conductivity, n is the porosity, ρ_w is the density of water, c_{pw} is the specific heat capacity of water, ρ_s is the density of sand and c_{ps} is the specific heat capacity of sand. More complex approaches for calculating thermal conductivity exist (De Vries, 1963). However, the above method is a reasonable approximation for low-permeabilities (Clauser, 2003; Saar and Manga, 2004; Walsh and Saar, 2010).

The thermal equilibrium distribution coefficient for linear heat sorption is the ratio of the specific heat of sand to the volumetric heat capacity of water (Hecht-Méndez et al., 2010):

$$K_d = \frac{c_{ps}}{\rho_w \times c_{pw}} \qquad (4)$$

where K_d is the distribution coefficient. This assumes instantaneous thermal equilibrium between the solid and liquid phases.

The physical properties of the BHE were divided into properties of the circulating fluid, properties of the grout surrounding the ground heat exchanger (GHE) tubes, and properties of the GHE tubes. For the simulations, water is used as the circulating fluid

and typical values are chosen for the properties of interest. Circulating fluids used in ground source heat pump systems are typically either water or a water/anti-freeze solution (2007 ASHRAE Handbook, 2007). A mixture of fine sand and 10% bentonite is used as the grout material in the BHE. Wang et al. (2013) recently found that this particular mixture improves the thermal performance of borehole heat exchangers and measured the thermal conductivity and density of this grout material. The specific heat capacity of the fine sand-bentonite grout was based on the values used by Florides et al. (2012) and Michopoulos and Kyriakis (2009). The BHE tube is modeled as a high-density polyethene U-tube, a standard tube used in GSHP systems (Choi, et al. 2013; Michopoulos and Kyriakis, 2009).

Table 1: Physical properties of aquifer and BHE.

Symbol	Property	Value	Units
Ground Properties (soil/rock, sand)			
k_s	Thermal conductivity, soil	1.67 0.835: half the k_s 2.51: 1.5 times the k_s	W/m/K
c_{ps}	Specific heat capacity, soil	703	J/kg/K
ρ_s	Density , soil	1415	kg/m^3
Ground Properties (aquifer)			
k_{eff}	Thermal conductivity, effective	1.51 0.800: half the k_s 2.21: 1.5 times the k_s	W/m/K
α	Thermal diffusivity, effective	1.025E-6 5.431E-7: half the k_s 1.507E-6: 1.5 times the k_s	m^2/s
K_d	Distribution coefficient	1.68E-4	m^3/kg
	Confined storage coefficient	0.001	
	Transmissivity	1E-3	m^2/s
n	Porosity	0.15	-
	Longitudinal dispersivity	0.50	m
	Horizontal transverse dispersivity	0.05	m
	Vertical transverse dispersivity	0.05	m
Borehole Heat Exchanger Properties (circulating fluid, water)			
k_w	Thermal conductivity, water	0.60	W/m/K
c_{pw}	Specific heat capacity, water	4180	J/kg/K
ρ_w	Density, water	1000	kg/m^3
μ_w	Dynamic viscosity, water	8.9045E-4	kg/m/s
u	Velocity of water in GHE tube	0.5	m/s
Borehole Heat Exchanger Properties (grout, fine sand-10% bentonite mixture)			
k_g	Thermal conductivity, grout	2.15	W/m/K
c_{pg}	Specific heat capacity, grout	830	J/kg/K
ρ_g	Density, grout	1568	kg/m^3
Borehole Heat Exchanger Properties (GHE tube, high-density polyethene U-tube)			
k_p	Thermal conductivity, GHE tube	0.4	W/m/K
r_{inn}	GHE tube inner radius	0.0215	m
r_{ext}	GHE tube outer radius	0.025	m
Borehole Heat Exchanger Properties			
L	Borehole length	100	m
r_b	Borehole radius	0.1	m

1.6. Comparison metrics

Several comparison metrics are used to evaluate the effects of thermal interference between BHEs and the impact of optimizing spacing between BHEs. In this study, the Péclet number, the percent change in BHE outlet temperature, and the percent change in BHE wall temperature are used in the evaluation.

1.6.1. The Péclet number

The Péclet number is defined as the ratio of the advective transport rate to the diffusive transport rate of heat. In other words, it relates the advective heat energy transport due to fluid flow to the conductive heat energy transport due to a temperature gradient. It is important, however, to keep in mind that for advective heat transport to have a measureable effect the fluid flow vector has to have a component that is parallel to the temperature gradient (Saar, 2011) as is given in the simulations presented here.

Domenico and Schwartz (1990) present the Péclet number Pe as follows:

$$\mathrm{Pe} = \frac{u\, l_c\, \rho_w\, c_{pw}}{k_{eff}} \qquad (5)$$

where u is the groundwater flow velocity, l_c is the characteristic length, ρ_w is the density of water, c_{pw} is the specific heat capacity of water, and k_{eff} is the effective thermal conductivity of the porous medium.

The characteristic length used to calculate the Péclet number must be consistent for comparisons between scenarios using Péclet numbers to be appropriate. Previous studies by Chiasson et al. (2000), Sutton et al. (2003), Diao et al. (2004), Molina-Giraldo et al. (2011) and Choi et al. (2013) have chosen various parameters as the characteristic lengths: the borehole spacing, the borehole radius, the radial distance from the borehole, the borehole length and a unit characteristic length. For the purposes of this study, a unit characteristic length was chosen for consistency between simulations to allow for easier comparison between simulations and previous work with varying parameters. This eliminates differences in Péclet numbers that arise from changes in the chosen characteristic length. Thus, characteristic lengths should be consistent to compare between simulations and studies.

1.6.2. Outlet temperature of the BHE

Michopoulos and Kyriakis (2009) developed an approach to calculate the circulating fluid outlet temperature for a vertical BHE (i.e., the temperature of the fluid upon exiting the BHE) based on the infinite line source model of Carslaw and Jaeger (1959) and the total thermal resistances of the BHE. The results were compared to actual experimental data and the differences were shown to be negligible. Below is an adaptation of their approach used to calculate the outlet temperature of the BHE following the simulation of the thermal response of the subsurface region outside the borehole.

The heat flux through the borehole wall is related to the temperature of the borehole wall and the temperature in the circulating fluid: $Q = A(T_w - T_b)/R_{tot}$. The model simulates the temperature at the interface between the borehole and the soil, T_b, and the circulating fluid temperature, T_w, at the BHE outlet can be calculated by knowing the total borehole thermal resistance, R_{tot}, and the specified heat flux, Q.

The total borehole thermal resistance, R_{tot}, includes the convection resistance between the fluid and the GHE tube, R_{con}, the convection resistance of the GHE tubes, R_p, and conduction resistance of the grout material, R_g,. The resistances are calculated as follows:

$$R_{tot} = R_{con} + R_p + R_g \qquad (6)$$

$$R_{con} = \frac{1}{a\,A} \qquad (7)$$

$$R_p = \frac{\ln\left(\frac{d_{ext}}{d_{inn}}\right)}{2\,\pi\,k_p\,L} \quad (8)$$

$$R_g = \frac{\ln\left(\frac{r_b}{d_{ext}}\right)}{2\,\pi\,k_g\,L} \quad (9)$$

where a is the convective heat transfer coefficient, A is the surface of convection, d_{ext} is the external diameter of the GHE tube, d_{inn} is the inner diameter of the GHE tube, r_b is the borehole radius, k_p is the thermal conductivity of the GHE tube material, k_g is the thermal conductivity of the grout material, and L is the length of the borehole.

The convective heat transfer coefficient is estimated using the Nusselt, Reynolds, and Prandtl numbers in the pipe (VDI Heat Atlas, 2010) as follows:

$$a = \frac{k_w}{2\,r_{inn}}\mathrm{Nu} \quad (10)$$

The Nussult number, Nu, is the ratio of convective to conductive heat transfer and can be calculated with the following equation:

$$\mathrm{Nu} = 0.023\,\mathrm{Re}^{0.8}\,\mathrm{Pr}^{n} \quad (11)$$

where n = 0.4 for heating applications (the borehole wall is hotter than the circulating fluid) and n = 0.33 for cooling applications (the borehole wall is cooler than the circulating fluid) from the VDI Heat Atlas (2010).

The Reynolds number, Re, is the ratio of inertial to viscous forces and can be calculated with the following equation:

$$\mathrm{Re} = \frac{\rho\, u\, d_{inn}}{\mu} \qquad (12)$$

where ρ is the fluid density, u is the fluid velocity, μ is the fluid dynamic viscosity and d_{inn} is the ground heat exchanger (GHE) tube inner diameter.

The Prandtl number, Pr, is the ratio of fluid momentum to thermal diffusivity and can be calculated with the following equation:

$$\mathrm{Pr} = \frac{\mu\, c_p}{\lambda} \qquad (13)$$

where μ is the fluid dynamic viscosity, c_p is the specific heat capacity, and λ is the thermal conductivity.

The surface of convection is calculated as follows:

$$A = 2\, L\, \pi\, d_{inn} \qquad (14)$$

The water temperature at the BHE outlet, $T_{w,}$ at time, $t,$ can then be calculated from the temperature simulated at the borehole wall, $T_{b,}$ and the temperature change caused by the constant heat flux of the BHE exchanger, $Q,$ by:

$$T_w(t) = T_b(t) - Q(t)\, R_{tot} \qquad (15)$$

1.6.3. The percent change in outlet and borehole wall temperatures

To evaluate the impact of heat advection on heat transport in ground source heat pump systems, the temperature of the circulating fluid at the heat exchanger outlet and the temperature at the borehole wall were compared at a range of Péclet numbers. The percent change in temperature that occurred from the case without groundwater flow to each case with groundwater flow was calculated using the following equation:

$$\text{Percent change} = \frac{T_{cond} - T_{adv}}{T_{cond}} \times 100 \quad (16)$$

A positive percent change indicates that the temperature at the outlet or borehole wall decreases with groundwater flow. A negative percent change indicates that the temperature at the outlet or borehole wall increases with groundwater flow.

2. Results and discussion

2.1. No thermal interactions between BHEs

MT3DMS simulations of a single BHE are used to investigate the effects of groundwater flow, operation time, and thermal diffusivity upon the heat exchange between the BHE and the aquifer and the thermal distribution in the aquifer for cases with no thermal interaction between BHEs. In these simulations, there is a single fully penetrating BHE with a constant heat injection of 25 W/m into the aquifer at the BHE, as discussed previously.

Between simulations, the groundwater flow velocity, length of operation and thermal diffusivity are varied. Ten groundwater flow velocities are simulated: 0 m/s, 5×10^{-9} m/s, 1×10^{-8} m/s, 5×10^{-8} m/s, 1×10^{-7} m/s, 5×10^{-7} m/s, 1×10^{-6} m/s, 5×10^{-6} m/s, 1×10^{-5} m/s, and 2.5×10^{-5} m/s. At each level of groundwater flow rate, simulations are run with subsurface effective (sand and water mixed) thermal diffusivities of 5.431×10^{-7} m^2/s, 1.025×10^{-6} m^2/s, and 1.507×10^{-6} m^2/s and (summer) cooling season operation lengths of 30 days, 90 days, and 180 days.

2.1.1. Effect of groundwater flow

As expected, at low groundwater flow velocities, heat advection does not significantly impact the conductive temperature distribution surrounding the single BHE. The temperature distribution remains similar to that for the case without groundwater flow until a threshold groundwater flow velocity is reached, as seen in Figure 2 and Figure 3. For these simulations, deviations from a conductive temperature distribution are apparent at, or above, minimum groundwater flow velocities of approximately 1 x 10^{-6} m/s to 5 x 10^{-6} m/s.

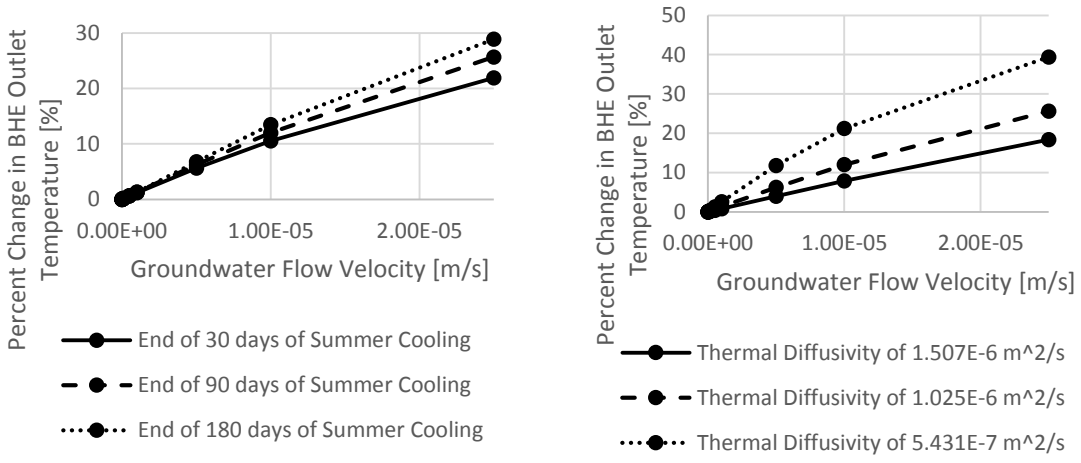

Figure 2. Effects of heat advection on the percent change in BHE outlet temperature for various a) season lengths and b) effective thermal diffusivities for a simulation of a single BHE and 90 days of summer cooling at 25 W/m.

Beyond the threshold groundwater flow velocity, with increased groundwater flow rates, less heat accumulates in the area immediately surrounding the BHE and the heat plume

extends farther from the BHE, as the heat is carried downstream of the BHE by the groundwater flow. This effect decreases the outlet temperature of the BHE necessary to input a constant amount of heat into the aquifer (Figure 2). Thus, the temperature drop from inlet to outlet of the circulating fluid is decreased for the constant heat exchange rate. The reduction in temperature drop with faster groundwater flow rates is consistent with the results of other studies (Diao et al., 2004; Fuji et al., 2005; Fan et al., 2007; Choi et al. 2013). Thus, the change in temperature decreases for the given heat transfer rate, indicating an increase in the overall efficiency of the GSHP system.

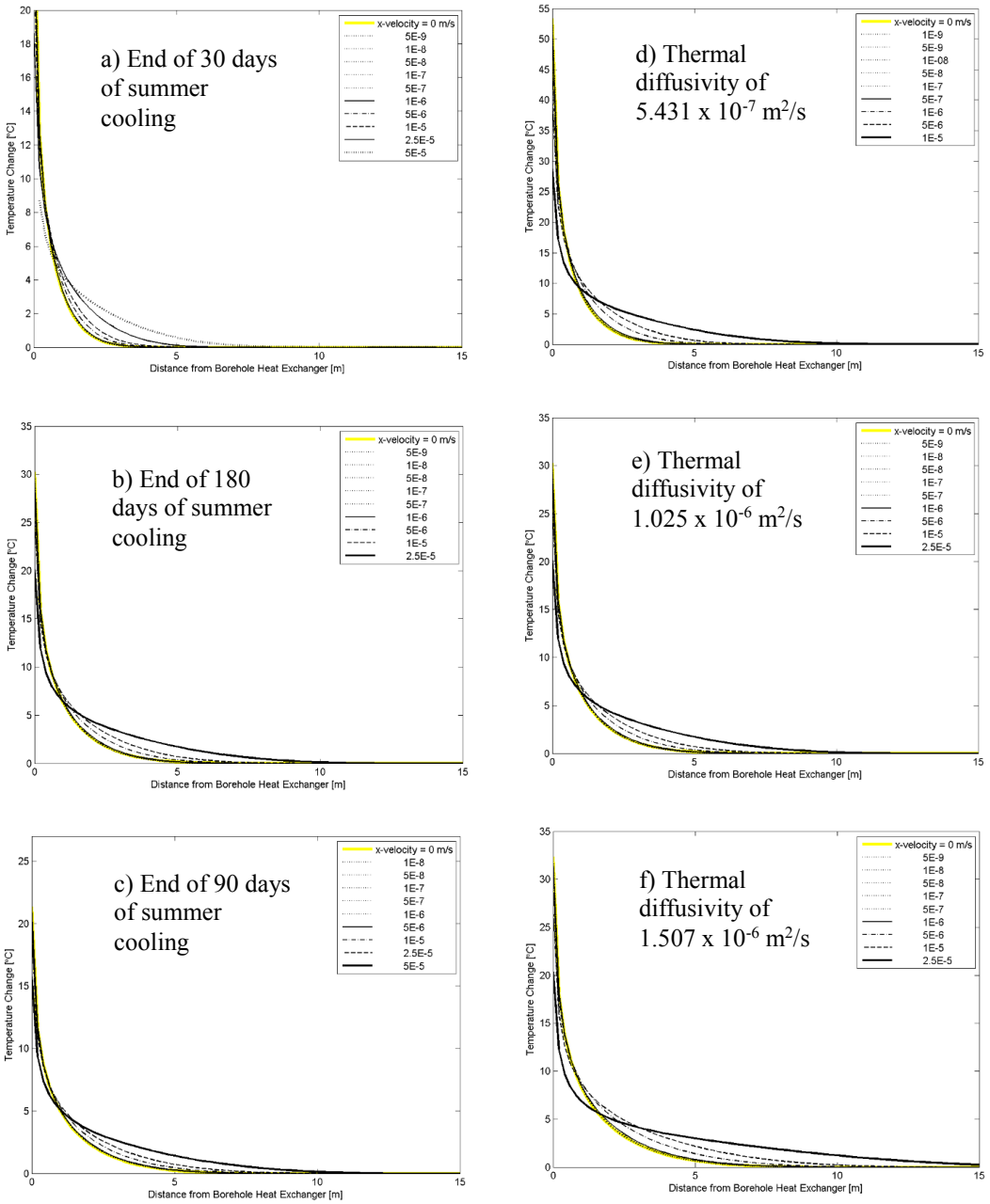

Figure 3. The temperature change in the aquifer surrounding a single BHE for various operation times: a) 30 days, b) 180 days, and c) 90 days of summer cooling at 25 W/m with thermal diffusivity of 1.025E-6 m2/s and various thermal diffusivities: d) 5.431E-7 m^2/s, e) 1.025E-6 m^2/s, and f) 1.507E-6 m^2/s after 90 days of summer cooling at 25 W/m.

2.1.2. Effect of operation time

As operation times increase (for example for a long summer cooling season), the importance of heat advection increases as it moves heat more efficiently than by conduction alone. At longer operation times, the heat accumulation (during summer operation) at the BHE is greater and the heat plume extends farther from the BHE at the end of the operation period as seen in Figure 3a for 30 days of operation, Figure 3b for 180 days of operation, and Figure 3c for 90 days of operation. Simulations of all levels of groundwater heat advection follow this trend. At longer operation times, the temperature gradient near the borehole decreases, which means the outlet circulating fluid temperature needs to increase for a given specified heat flux.

The rate of groundwater heat advection appears to have approximately the same impact on GSHP systems with 30, 90, and 180 days of continuous operation, as increasing or decreasing the duration of operation did not change the threshold groundwater flow velocity at which BHE outlet temperature significantly changed. Table 2 shows the groundwater flow velocities at which a 1% and 5% decrease in BHE outlet temperature occurs, compared to the conduction only case. A 1% decrease in BHE temperature occurs at a groundwater flow velocity between 5×10^{-7} m/s and 1×10^{-6} m/s for the shortest operation length (30 days), between 1×10^{-6} m/s and 5×10^{-6} m/s for the intermediate operation length (90 days), and 5×10^{-7} m/s and 1×10^{-6} m/s for the longest operation

length (180 days). The range in Péclet numbers associated with the threshold groundwater flow velocities vary little with operation length (Table 2).

Table 2. Threshold groundwater flow velocities and Péclet numbers for significant changes in BHE outlet temperatures in single BHE simulations with a thermal diffusivity of 1.025E-6 m^2/s and either 30, 90, or 180 days of cooling (during summer operation).

	1% change in BHE outlet temperature			**5% change in BHE outlet temperature**		
Days of operation	**Groundwater x-velocity [m/s]**	**Percent change**	**Péclet number**	**Groundwater x-velocity [m/s]**	**Percent change**	**Péclet number**
30	5E-7 – 1E-6	0.61 – 1.2	1.4 – 2.8	1E-6 – 5E-6	1.2 – 5.6	2.8 – 14
90	1E-6 – 5E-6	0.32 – 2.3	2.8 – 14	5E-6 – 1E-5	2.3 – 5.7	14 - 28
180	5E-7 – 1E-6	0.65 – 1.3	1.4 – 2.8	1E-6 – 5E-6	1.3 – 6.8	2.8 - 14

Based on Appendix B: Table 9, Table 10, and Table 11.

GSHP systems with various operation durations have the potential to benefit from the consideration of groundwater heat advection. The simulations show that heat build-up near the BHE is significantly reduced at a similar range of groundwater flow velocities at operation lengths of 30, 90, and 180 days. Beyond the threshold groundwater flow velocity, as the duration of the summer cooling season in increased from 30 days to 180 days, the outlet circulating fluid temperature of the BHE is more significantly reduced (Figure 2). Thus, the temperature drop from inlet to outlet of the circulating fluid is

decreased for the constant heat exchange rate. Lower temperature drops in circulating fluid enhances GSHP system performance and allows for greater efficiency in system operation. This potentially reduces the number of installed BHEs when considered during the design stages.

2.1.3. Effect of effective thermal diffusivity

As thermal diffusivities increase, the importance of groundwater advection decreases as heat conduction becomes more efficient. For a given groundwater flow velocity, an increase in thermal diffusivity results in less heat accumulation near the BHE and conductive spreading of the heat plume from the BHE over a larger extent as seen in Figure 3d,e, and f for thermal diffusivities of 5.431×10^{-7} m^2/s, 1.025×10^{-6} m^2/s, and 1.507×10^{-6} m^2/s, respectively. Simulations of all levels of groundwater heat advection followed this trend. Conversely, in areas with low thermal diffusivities, more heat builds up near the BHE as it conducts only over relatively shorter distances in the same time period with a characteristic travel distance given by $d = \sqrt{\alpha\, t}$ where d is the distance, α is the diffusivity and t is the time.

Due to the increased heat accumulation near the BHE at lower thermal diffusivities, groundwater heat advection has more impact on GSHP systems located in aquifers with lower effective thermal diffusivities (Figure 2).

Table 3 shows the groundwater flow velocities necessary to create a 1% and 5% decrease in BHE outlet temperature compared to the conduction only case. A 1% decrease in BHE temperature occurs at a groundwater flow velocity between 1 x 10^{-7} m/s and 5 x 10^{-7} m/s for the lowest thermal diffusivity (5.431 x 10^{-7} m^2/s), between 5 x 10^{-7} m/s and 1 x 10^{-6} m/s for the intermediate thermal diffusivity (1.025 x 10^{-6} m^2/s), and between 1 x 10^{-6} m/s and 5 x 10^{-6} m/s for the highest thermal diffusivity (1.507 x 10^{-6} m^2/s). The range in Péclet numbers associated with these threshold velocities are approximately the same for each of the thermal diffusivities as they depend both on thermal diffusivity and groundwater flow velocity (Table 3).

Table 3. Threshold groundwater velocities and Péclet numbers for significant changes in BHE outlet temperatures for single BHE simulations after 90 days of cooling with a thermal diffusivity of 5.431E-7 m^2/s, 1.025E-6 m^2/s or 1.507E-6 m^2/s.

	1% change in BHE outlet temperature			**5% change in BHE outlet temperature**		
Thermal diffusivity [m^2/s]	**Groundwater x-velocity [m/s]**	**Percent change**	**Péclet number**	**Groundwater x-velocity [m/s]**	**Percent change**	**Péclet number**
5.431E-7	1E-7 – 5E-7	0.26 – 1.3	0.52 – 2.6	1E-6 – 5E-6	2.6 – 12	5.2 – 26
1.025E-6	5E-7 – 1E-6	0.68 – 1.3	1.4 – 2.8	1E-6 – 5E-6	1.3 – 6.2	2.8 – 14
1.507E-6	1E-6 – 5E-6	0.75 – 3.9	1.9 – 9.4	5E-6 – 1E-5	3.9 – 7.9	9.4 - 19

Based on Appendix B: Table 9, Table 12 and Table 13.

Beyond the threshold groundwater flow velocity, as the effective thermal diffusivity decreases from 1.507 x 10^{-6} m^2/s to 5.431 x 10^{-7} m^2/s, the outlet circulating fluid temperature of the BHE is more significantly reduced (Figure 2). Thus, the temperature drop from inlet to outlet of the circulating fluid is decreased for the constant heat exchange rate. Lower temperature drops in circulating fluid enhances GSHP system performance and allows for greater efficiency in system operation. This allows for greater efficiency in system operation and potentially the reduction of installed BHEs when considered during the design stages.

When considering the thermal diffusivity of a GSHP, it is important to note the difference between the thermal diffusivity in the unsaturated zone, above the groundwater table (where air fills the pores), and the saturated zone, below the groundwater table (where groundwater fills the pores). With air filled pores, the effective thermal conductivity, 1.42 W/m/K, is lower than that with water filled pores, 1.51 W/m/K. However, the effective thermal diffusivity of the unsaturated zone, 1.683 x 10^{-6} m^2/s, is higher than that of the saturated zone, 1.025 x 10^{-6} m^2/s, due to the low volumetric heat capacity of air. This means that heat will move more rapidly through the unsaturated zone. However, given the low heat capacity in the unsaturated zone, much less heat can be stored and heat build-up or freezing occurs more quickly in the unsaturated zone. Therefore, it is generally advisable to place the BHEs below the groundwater table when feasible.

Areas with higher thermal diffusivities may also benefit from the consideration of groundwater heat advection. However, significant reductions in heat build-up will only occur in areas with faster groundwater flow. A combined threshold of thermal diffusivity and groundwater flow velocity exists beyond which there are potential gains in GSHP system efficiency due to consideration of groundwater flow rats. The threshold Péclet number associated with a 1% change in BHE outlet temperature is approximately 2 for each thermal diffusivity and approximately 11 for a 5% change in BHE outlet temperature.

2.2. Thermal interactions among multiple BHEs

MT3DMS simulations of three BHEs situated parallel to the direction of groundwater flow (as seen in Figure 1) are used to investigate the effects of groundwater flow, operation time, and thermal diffusivity on the heat exchange between the BHE and the aquifer and the thermal distribution in the aquifer for cases with thermal interaction between heat exchangers. In these simulations, there are three BHEs each with a constant heat exchange of 25 W/m at the BHEs.

Between simulations the groundwater flow velocity, length of operation and thermal diffusivity are varied. As before, ten groundwater flow velocities are simulated: 0 m/s, 5 x 10^{-9} m/s, 1 x 10^{-8} m/s, 5 x 10^{-8} m/s, 1 x 10^{-7} m/s, 5 x 10^{-7} m/s, 1 x 10^{-6} m/s, 5 x 10^{-6} m/s, 1 x 10^{-5} m/s, and 2.5 x 10^{-5} m/s. For each groundwater flow velocity, simulations are run with the following thermal diffusivities: 5.431 x 10^{-7} m^2/s, 1.025 x 10^{-6} m^2/s, and 1.507 x 10^{-6} m^2/s and (summer) cooling season operation lengths of 30 days, 90 days, and 180 days.

2.2.1. Effect of groundwater flow

At low groundwater flow velocities, including heat advection does not significantly impact the temperature distribution surrounding the three BHEs, as seen before in Section 2.1.1. The temperature distribution remains similar to the case without groundwater flow until a threshold groundwater flow velocity is reached, as seen in Figure 4 and Figure 5. For these simulations, deviations from a conductive temperature distribution are apparent at minimum groundwater flow velocities of approximately $1x10^{-6}$ m/s to $5x10^{-6}$ m/s.

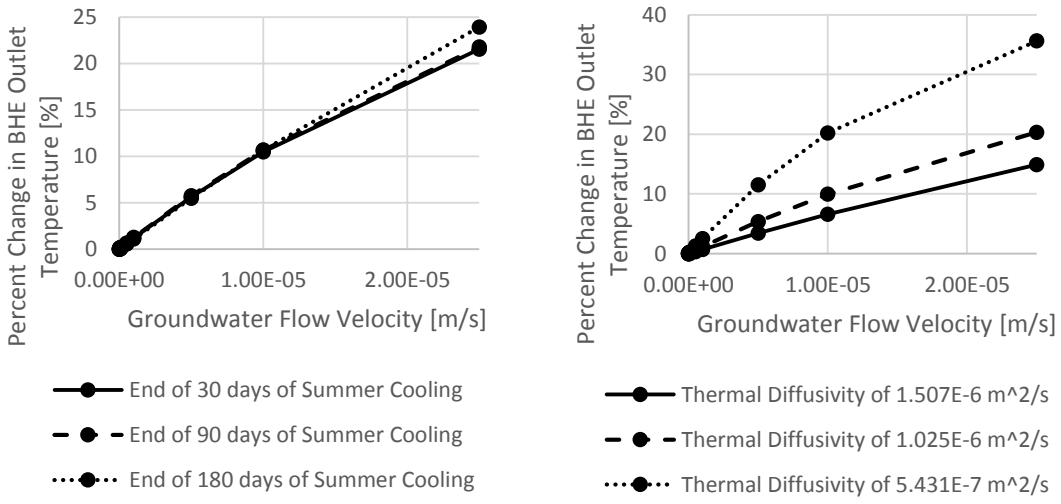

Figure 4. Effects of heat advection on the percent change in BHE outlet temperature for various a) season lengths and b) effective thermal diffusivities for simulations with three BHES and 90 days of summer cooling at 25 W/m.

Beyond the threshold groundwater flow velocity, with increased groundwater flow less heat accumulates in the area immediately surrounding the BHEs and the heat plume extends farther from each BHE. Heat transfer between the heat exchanger and the aquifer

is increased, causing the percent change of the BHE outlet temperature to decrease as compared to the conductive case (Figure 4). Additionally, the temperature drop of the circulating fluid between the inlet and outlet of the BHE is lowered at faster groundwater flow rates, which increases the overall efficiency of the GSHP system.

At higher groundwater flow velocities, the heat injected into the aquifer is carried to the next BHE within the 90 day summer cooling season. This actually increases the temperature of the BHE fluid necessary for a constant heat transfer of 25 W/m. For example, after 90 days of summer cooling at a heat transfer rate of 25 W/m and a thermal diffusivity of 1.025×10^{-6} m^2/s, at a groundwater flow velocity of 2.5×10^{-6} m^2/s the temperature at the first BHE outlet is 29.33 °C, at the second BHE outlet is 31.08 °C and at the third is 31.22 °C (Appendix C: Table 14). This effect is less significant for lower groundwater flow velocities. So for systems employing a standardized spacing between BHEs, heat advection through groundwater flow can cause negative thermal interactions between BHEs. By simulating the GSHP systems and choosing an optimum spacing between BHEs, as is the premise of this study, the negative thermal interactions between BHEs may be eliminated.

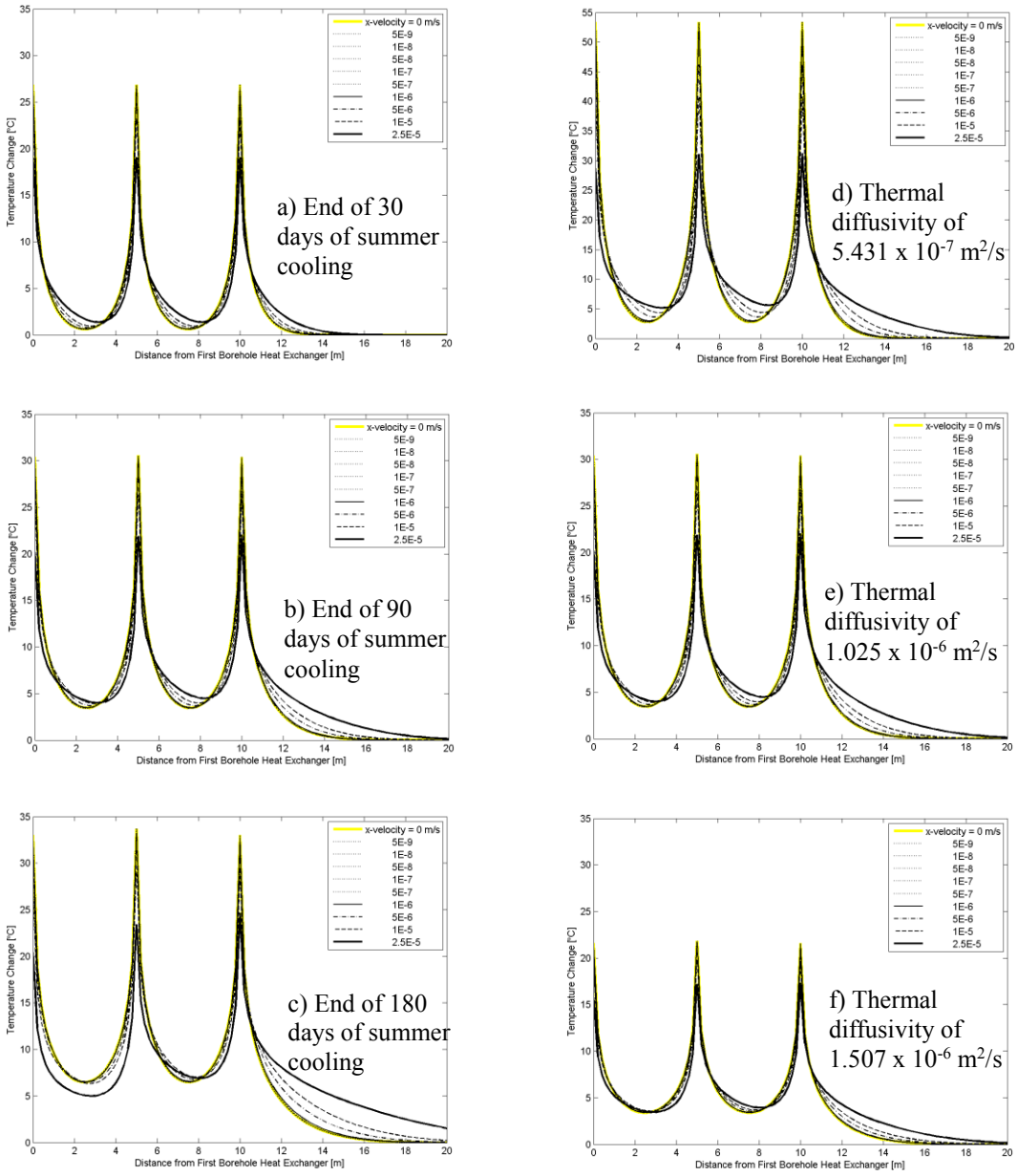

Figure 5. The temperature change in the aquifer surrounding three BHEs for various operation times: a) 30 days, b) 90 days, and c) 180 days of summer cooling at 25 W/m with thermal diffusivity of 1.025E-6 m2/s and various thermal diffusivities: d) 5.431E-7 m^2/s, e) 1.025E-6 m^2/s, and f) 1.507E-6 m^2/s after 90 days of summer cooling at 25 W/m.

2.2.2. Effect of operation time

As operation times increase, the importance of heat advection increases as the heat accumulation at a given BHE is greater and the heat plume extends farther from the BHE at the end of the operation period as seen in Figure 5a, b, and c for 30 days of operation, 90 days of operation, and 180 days of operation, respectively. Subsequently, the longer operation times lead to a greater build-up of heat between the three simulated heat exchangers. Simulations of all levels of groundwater heat advection follow this trend.

At higher groundwater flow velocities there is an increase in BHE outlet temperature along the groundwater flow path as heat from one BHE is advected to the adjacent BHE within the summer cooling season. This effect is minimal for a 30 day season with a thermal diffusivity of 1.025×10^{-6} m^2/s (see Appendix C: Table 15), but is significant for a 90 day and 180 days season with the same thermal diffusivity. After 90 days of summer cooling, BHE outlet temperatures are increased at groundwater flow levels of 1×10^{-5} m/s and higher (Appendix C: Table 15). The rise in temperature is within 2 °C between the three BHEs at the highest groundwater flow velocity simulated. After 180 days of summer cooling, BHE outlet temperature are increased at groundwater flow levels of 5×10^{-8} m/s and higher (Appendix C: Table 16), which is significantly lower than the threshold groundwater flow velocity after 90 days. The rise in temperature is over 4 °C between the three BHEs at the highest groundwater flow velocity simulated. Therefore, negative thermal interference increases with the duration of BHE operation.

Table 4. Threshold groundwater velocities and Péclet numbers for significant changes in BHE outlet temperatures for three BHE simulations with a thermal diffusivity of 1.025E-6 m^2/s and either 30, 90 or 180 days of cooling.

	1% change in BHE outlet temperature			**5% change in BHE outlet temperature**		
Days of operation	**Groundwater x-velocity [m/s]**	**Percent change**	**Péclet number**	**Groundwater x-velocity [m/s]**	**Percent change**	**Péclet number**
30	5E-7 – 1E-6	0.61 – 1.2	1.4 – 2.8	1E-6 – 5E-6	1.2 – 5.6	2.8 – 14
90	5E-7 – 1E-6	0.65 – 1.3	1.4 – 2.8	1E-6 – 5E-6	1.3 – 5.8	2.8 – 14
180	5E-7 – 1E-6	0.60 – 1.1	1.4 – 2.8	1E-6 – 5E-6	1.1 – 5.5	2.8 – 14

The percent change in temperature was evaluated at the center BHE.

Based on Appendix C: Table 14, Table 15 and Table 16.

As in Section 2.1.2, groundwater heat advection appears to have approximately the same impact on GSHP systems with 30, 90 and 180 days of continuous operation. Increasing or decreasing the length of operation did not change the threshold groundwater flow velocity at which BHE outlet temperature significantly changed. Table 4 shows the groundwater flow velocities at which a 1% and 5% decrease in BHE outlet temperature compared to the conduction only case occur. For all three operation lengths (30, 90 and 180 days), a 1% decrease in BHE temperature occurred at a groundwater flow velocity between 5 x 10^{-7} m/s and 1 x 10^{-6} m/s. For the case of three BHEs spaced 5 meters from

each other, the threshold Péclet numbers, between 1.4 and 2.8 when a unit characteristic length is used, are the same for each season duration (Table 4).

2.2.3. Effect of effective thermal diffusivity

As thermal diffusivities decrease, the importance of groundwater advection increases. At higher thermal diffusivities, less heat accumulates near each BHE and the extent of the heat plumes from the BHEs increases slightly as seen in Figure 5d, e, and f for a thermal diffusivity of 5.431 x 10^{-7} m^2/s, 1.025 x 10^{-6} m^2/s, and 1.507 x 10^{-6} m^2/s, respectively. High thermal diffusivities allow heat to conduct away from the BHEs more rapidly than occurs at lower thermal diffusivities.

Above a certain threshold groundwater flow velocity, BHE outlet temperature increases from BHE to BHE along the groundwater flow path. Heat from one BHE is advected to the adjacent BHE within a single summer cooling season. This effect is significant for the thermal diffusivities simulated and is greater at lower thermal diffusivities. For the highest (1.507 x 10^{-6} m^2/s) and the intermediate thermal diffusivity (1.025 x 10^{-6} m^2/s), the effect occurs at groundwater flow velocities of 5 x 10^{-7} m/s and higher and the rise in temperature is within 2 °C between the three BHEs at the highest groundwater flow velocity simulated (Appendix C: Table 14 and Table 18). For the lowest thermal diffusivity (5.431 x 10^{-7} m^2/s), the effect occurs at groundwater flow velocities of 5 x 10^{-7} m/s and higher and the rise in temperature is within 3 °C between the three BHEs at the highest groundwater flow velocity simulated (Appendix C: Table 17). The threshold groundwater flow velocities are the same between the three thermal diffusivities, but the temperature increases at the BHEs are greater at the lowest thermal diffusivity (5.431 x

10^{-7} m^2/s). Therefore, the impact of negative thermal interference is greater at lower thermal diffusivities.

Table 5. Threshold groundwater velocities and Péclet numbers for significant changes in BHE outlet temperatures for three BHE simulations after 90 days of operation with a thermal diffusivity of 5.431E-7 m^2/s, 1.025E-6 m^2/s or 1.507E-6 m^2/s.

	1% change in BHE outlet temperature			**5% change in BHE outlet temperature**		
Thermal diffusivity [m^2/s]	**Groundwater x-velocity [m/s]**	**Percent change**	**Péclet number**	**Groundwater x-velocity [m/s]**	**Percent change**	**Péclet number**
5.431E-7	5E-8 – 1E-7	0.26 – 1.3	0.52 – 2.6	1E-6 – 5E-6	2.5 – 12	5.2 – 23
1.025E-6	5E-7 – 1E-6	0.65 – 1.3	1.4 – 2.8	1E-6 – 5E-6	1.3 – 5.8	2.8 – 14
1.507E-6	1E-6 – 5E-6	0.68 – 3.4	1.9 – 9.5	5E-6 – 1E-5	3.4 – 6.6	9.5 – 19

The percent change in temperature was evaluated at the center BHE.

Based on Appendix C: Table 14, Table 17 and Table 18.

As in Section 2.1.3, due to the increased heat accumulation near each BHE at lower thermal diffusivities, groundwater heat advection has more impact on GSHP systems located in aquifers with lower thermal diffusivities (Figure 4). Table 5 shows the groundwater flow velocities that cause a 1% and 5% decrease in BHE outlet temperature in the center BHE compared to the conduction only case. A 1% decrease in BHE temperature occurs at a groundwater flow velocity between 5 x 10^{-8} m/s and 1 x 10^{-7} m/s for the lowest thermal diffusivity (5.431 x 10^{-7} m^2/s), between 5 x 10^{-7} m/s and 1 x 10^{-6}

m/s for the intermediate thermal diffusivity (1.025 x 10^{-6} m^2/s), and between 1 x 10^{-6} m/s and 5 x 10^{-6} m/s for the highest thermal diffusivity (1.507 x 10^{-6} m^2/s). A combined threshold of thermal diffusivity and groundwater flow velocity exists beyond which there are potential gains in GSHP system efficiency. The threshold Péclet number associated with a 1% change in BHE outlet temperature is approximately 2 and with a 5% change in BHE outlet temperature is approximately 11 for each thermal diffusivity (Table 5).

Beyond the threshold groundwater flow velocity, as the effective thermal diffusivity decreases from 1.507 x 10^{-6} m^2/s to 5.431 x 10^{-7} m^2/s, the outlet circulating fluid temperature of the center BHE also decreases as compared to the conductive case (Figure 4). Thus, the temperature drop from inlet to outlet of the circulating fluid is decreased for the constant heat exchange rate applied at the BHE.

This effect is lower in GSHP systems with thermal interference between multiple BHEs than in the systems without thermal interference previously discussed (Section 2.1.3 and Figure 2), particularly at the fastest groundwater flow rate simulated. For a groundwater flow velocity of 2.5 x 10^{-6} m/s, the percent change in BHE outlet temperature is approximately 3% lower for systems with thermal interference, a change of 10-20% depending on the effective thermal diffusivity of the system. This is due to the heat advection from an upstream BHE to the adjacent downstream BHE, the negative thermal interference.

2.3. Optimization of BHE spacing

2.3.1. Determine BHE spacing for optimization

The first step to optimizing the placement of BHEs in the GSHP system is to determine the distance that heat is transported in half a year (assuming constant groundwater flow velocities or half-year average groundwater flow velocity) so that it can be utilized in the next operation season. For large-scale system installations, a year-long (or even multi-year investigation of the groundwater flow velocity filed could be beneficial. Once, groundwater flow velocities are determined, excess heat injected into the aquifer during a (summer) cooling season could be captured for use in the following (winter) heating season. Conversely, a cold plume, generated during a (winter) heating season could increase the efficiency of heat transfer from a BHE into the aquifer during the following (summer) cooling season. In order to maximize such positive interference between BHEs, the BHEs must be installed at a specific distance apart so that the maximum (or minimum) temperatures in the aquifer reaches the adjacent BHE during the following heating (or cooling) season.

This distance is determined by simulating a series of four seasons representing a one year cycle of heating and cooling: a 90 day summer cooling season, a 90 day fall no operation season, a 90 days winter heating season and then a 90 day spring no operation season. Each half year is considered separately when determining these distances.

The first half year considers the summer cooling season (Figure 6a) in which 10 W/m is injected at the BHE into the aquifer and the fall no operation season (Figure 6b). The distance from the BHE to the peak temperature at the end of the second season (as seen in Figure 6b) is the distance heat is transported in a half year, under the conditions of the GSHP field. The peak temperature (build up) occurs at the BHE for groundwater flow velocities at and below 1 x 10^{-6} m/s (Table 6), i.e., when advective heat transfer away from the BHE is negligible. For these simulations, there is no spacing between BHEs that will allow for the utilization of the previous season's heat injection or extraction. The placement of these BHEs should be determined based upon minimizing the negative interference between the BHEs. Oftentimes, industry standard spacing is applied to these systems, but the spacing can also be chosen based upon the distance heat advects from the BHE, as illustrated in these simulations and further discussed below.

Table 6. Distance from the BHE to peak and minimum temperatures after a half year and full year of operation.

Groundwater x-velocity [m/s]	**Distance from BHE to temperature maximum, Season 2 [m]**	**Distance from BHE to temperature maximum, Season 4 [m]**	**Distance from BHE to temperature minimum, Season 4 [m]**
0	0	7.4	0
1E-6	0	7	0
5E-6	1.3	8.2	1
1E-5	2.8	10.8	2.2
2.5E-5	6.9	18.6	6.4
5E-5	13.8	34.8	13.8

Based on Appendix D: Table 20 and Table 22.

The peak temperature occurs 1.3 m from the BHE at a groundwater flow velocity of 5 x 10^{-6} m/s, 2.8 m from the BHE at a groundwater flow velocity of 1 x 10^{-5} m/s, 6.9 m from the BHE at a groundwater flow velocity of 2.5 x 10^{-5} m/s, and 13.8 m from the BHE at a groundwater flow velocity of 5 x 10^{-5} m/s as shown in Table 6.

At the lower groundwater flow velocities (5 x 10^{-6} m/s and 1 x 10^{-5} m/s), the peak temperature occurs too close to the BHE to utilize the heat injected into the aquifer at the start of the next (winter) heating season when heat is extracted from the subsurface. The interference between BHEs at these distances is significant enough to negate the effects of placing the BHE within the hot or cold plume as seen in Figure 6b. It may be possible to place the BHEs a year and a half apart, as opposed to a half year apart, to work around this limitation. However, when following this approach, the amplitude of the heat signal will be damped and the peak will be broadened. Thus, multi-year simulations would have to be carried out to investigate if such a strategy improves results. For the two higher groundwater flow velocities investigated (2.5 x 10^{-5} m/s and 5 x 10^{-5} m/s), the peak temperature occurs at a distance (6.65 m and 13.8 m, respectively) appropriate for utilizing the previous season's heating or cooling load.

In determining the optimal BHE spacing, the distances found above are averaged with the corresponding distances from the second half of the year. This half year consists of a 90 day season of winter heating during which a constant heat flux of 10 W/m is extracted at the BHE followed by a 90 day spring season with no operation. The distance heat is

transported in half a year under the conditions of the GSHP field is the distance from the BHE to the minimum temperature at the end of the fourth season (as seen in Figure 6d).

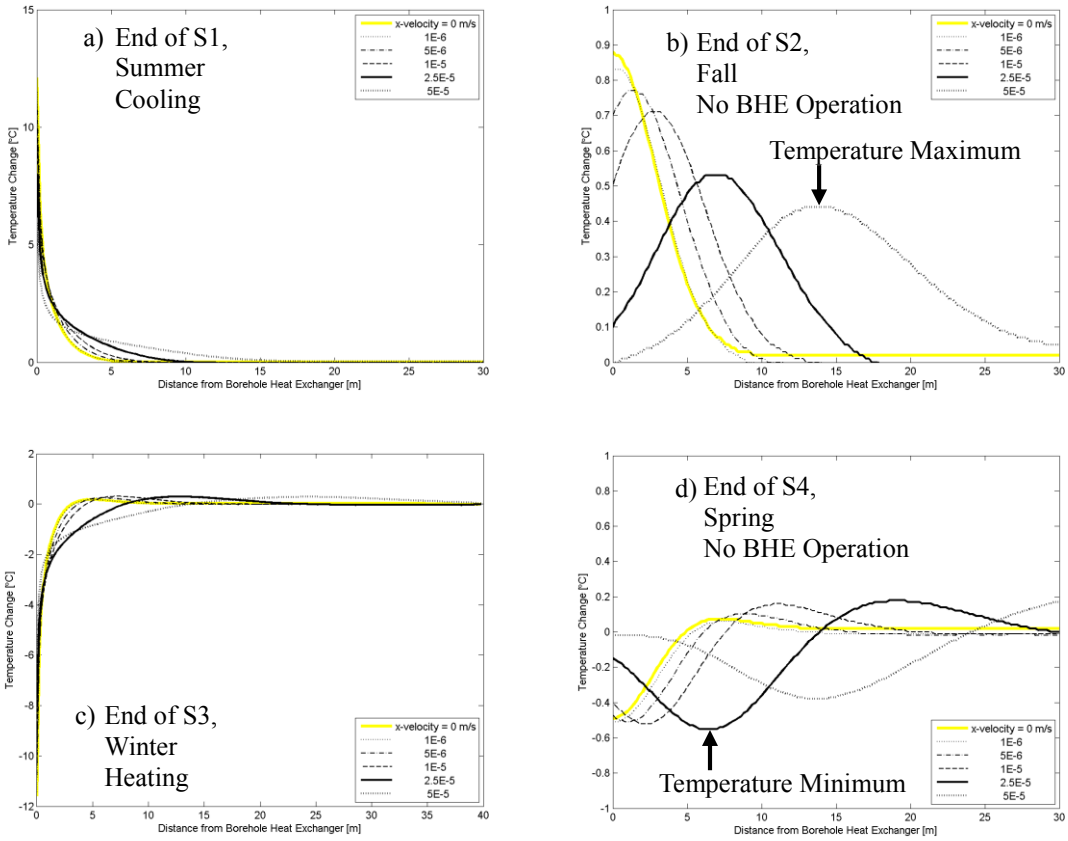

Figure 6. A time series of the temperature change in the aquifer with a thermal diffusivity of 1.025E-6 m^2/s surrounding a single BHEs during a one year heating and cooling cycle. a) End of Season 1: After 90 days of summer cooling at a constant heat transfer rate of 10 W/m, b) End of Season 2: After 90 days of no BHE operation, c) End of Season 3: After 90 days of winter heating at a constant heat transfer rate of 10 W/m, d) End of Season 4: After 90 days of no BHE operation.

Similar to the first half year, the temperature minimum occurs at the BHE for groundwater velocities at and below 1 x 10^{-6} m/s which is shown in Table 6. For these simulations, there is no displacement between BHEs that will allow for the utilization of the previous season's heat injection or extraction. The peak temperature occurs 1.0 m from the BHE at a groundwater velocity of 5 x 10^{-6} m/s, 2.2 m from the BHE at a groundwater velocity of 1 x 10^{-5} m/s, 6.4 m from the BHE at a groundwater velocity of 2.5 x 10^{-5} m/s and 13.8 m from the BHE at a groundwater velocity of 5 x 10^{-5} m/s as shown in Table 6.

After averaging, the BHE spacing for optimization is 1.15 m at a groundwater velocity of 5 x 10^{-6} m/s, 2.5 m at a groundwater velocity of 1 x 10^{-5} m/s, 6.65 m at a groundwater velocity of 2.5 x 10^{-5} m/s and 13.8 m at a groundwater velocity of 5 x 10^{-5} m/s as shown in Table 6. As discussed previously, beyond a certain minimum groundwater flow velocity, advective heat transfer significantly affects the transport of heat in a GSHP system. At the threshold minimum groundwater flow velocity, the effects of heat advection become dominant to the effects of heat conduction at a level significant enough for the advective heat transport away from the BHE to become apparent. This occurs at a Péclet number of approximately 2.8 during the summer cooling season, 4.5 during the fall no operation season, 0.89 during the winter heating season, and 37 for the spring no operation season.

Table 7 shows the groundwater flow velocities at which a 1% and 5% decrease in BHE outlet temperature occur compared to the conduction only case. For the first season, a 1% decrease in BHE temperature occurs at a groundwater flow velocity between 5 x 10^{-7} m/s and 1 x 10^{-6} m/s. For the second season, a 1% decrease in BHE temperature occurs at a groundwater flow velocity between 1 x 10^{-6} m/s and 5 x 10^{-6} m/s. For the third season, a 1% decrease in BHE temperature occurs at a groundwater flow velocity between 1 x 10^{-7} m/s and 5 x 10^{-7} m/s. For the fourth and final season, a 1% decrease in BHE temperature occurs at a groundwater flow velocity between 1 x 10^{-5} m/s and 2.5 x 10^{-5} m/s.

Table 7. Threshold groundwater flow velocities and Péclet numbers for significant changes in BHE wall temperatures for single BHE simulations at the end of four 90 day seasons of operation.

	1% change in BHE wall temperature			**5% change in BHE wall temperature**		
	Groundwater x-velocity [m/s]	**Percent change**	**Péclet number**	**Groundwater x-velocity [m/s]**	**Percent change**	**Péclet number**
S1: Summer Cooling at 10 W/m	5E-7 – 1E-6	0.56 – 1.0	1.4 – 2.8	5E-6 – 1E-5	4.1 – 7.9	14 – 28
S2: Fall No BHE Operation	1E-6 – 5E-6	0.39 – 1.4	2.8 – 14	1E-5 – 2.5E-5	3.0 – 6.1	28 – 69
S3: Winter Heating at 10 W/m	1E-7 – 5E-7	2.4 – -14	0.28 – 1.4	1E-7 – 5E-7	2.4 – -14	0.28 – 1.4
S4: Spring No BHE Operation	1E-5 – 2.5E-5	-0.78 – -3.0	28 – 69	> 1E-4	< -4.2	> 280

Based on Appendix D: Table 19, Table 20, Table 21 and Table 22.

The Péclet numbers associated with the 1% change in BHE wall temperature increases markedly during the fall (second) season and the spring (fourth) season (Table 7). During seasons of summer cooling and winter heating (Figure 6a and c) a significant difference in BHE temperature occurs at lower groundwater flow velocities which does not occur during the fall and spring seasons (Figure 6b and d). In all seasons, the peak and minimum temperatures are larger in magnitude and the plume extends farther from the peak (or minimum) at higher groundwater velocities.

2.3.2. Simulations with optimal BHE spacing after two years of operation

Based upon the BHE spacing determined in the previous section, four BHEs are placed parallel to the direction of groundwater flow (as seen in Figure 1). Two years of GSHP operation are simulated with four seasons per year: 90 days of summer cooling at a constant heat transfer rate of 10 W/m, 90 days of no BHE operation, 90 days of winter heating at a constant heat transfer rate of 10 W/m and 90 days of no BHE operation. The BHE spacing for optimization is 13.8 m at a groundwater flow velocity of 5 x 10^{-5} m/s, 6.65 m at a groundwater flow velocity of 2.5 x 10^{-5} m/s and 2.5 m at a groundwater flow velocity of 1 x 10^{-5} m/s.

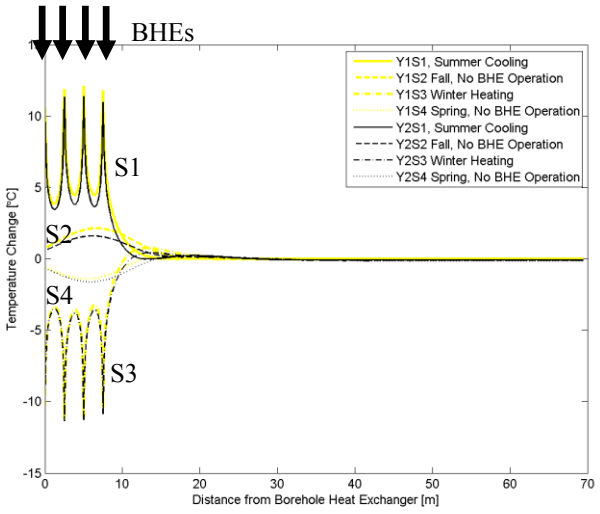

Figure 7. The temperature change in the aquifer surrounding four BHEs spaced optimally with a thermal diffusivity of 1.025E-6 m^2/s and a groundwater velocity of 1 x 10^{-5} m/s. *The model simulates two years of operation with four seasons: 90 days of cooling at a constant heat transfer rate of 10 W/m, 90 days of no BHE operation and 90 days of heating at a constant heat transfer rate of 10 W/m.*

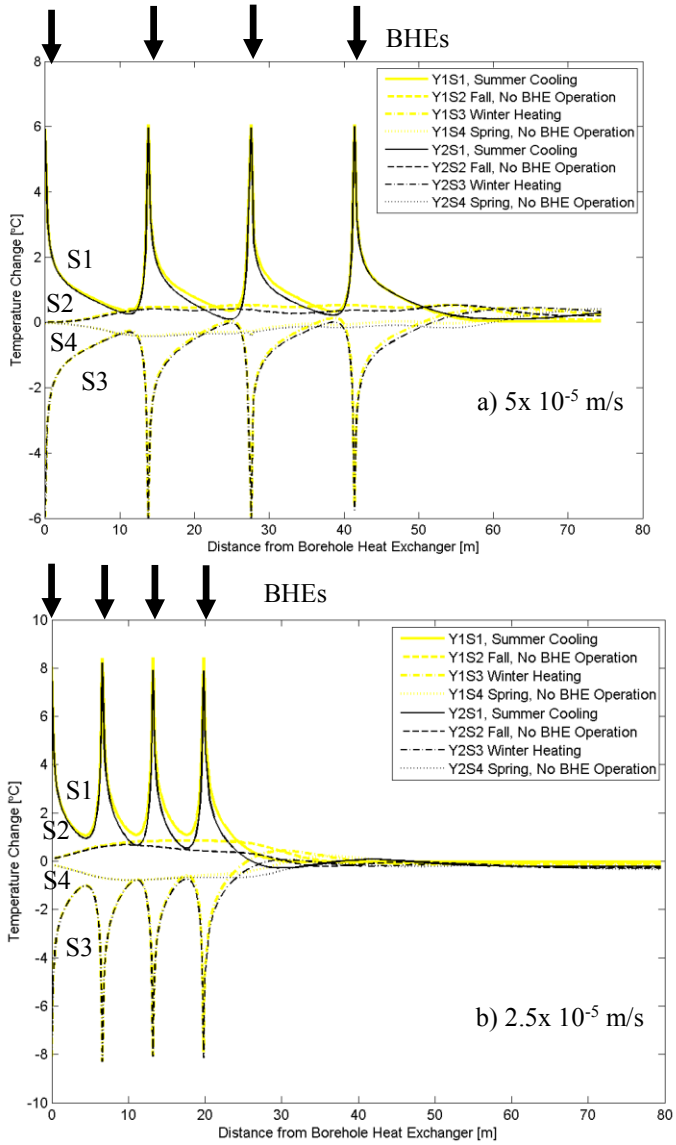

Figure 8. The temperature change in the aquifer surrounding four BHEs spaced optimally with a thermal diffusivity of 1.025 x 10^{-6} m^2/s and a groundwater velocity of a) 5 x 10^{-5} m/s *and b) 2.5* x 10^{-5} m/s. *The model simulates two years of operation with four seasons: 90 days of cooling at a constant heat transfer rate of 10 W/m, 90 days of no BHE operation and 90 days of heating at a constant heat transfer rate of 10 W/m.*

For the 5 x 10^{-5} m/s and 2.5 x 10^{-5} m/s groundwater flow velocity simulations, the optimization of BHE spacing allows for the capture of temperature peaks and minimums for the next operation season and the reduction of heat build-up (or freezing) in the BHE field as seen in Figure 8. For the lowest groundwater flow velocity simulation (1 x 10^{-5}

m/s), the peak temperature occurs too close to the BHE to utilize the heat extracted or injected into the aquifer at the start of the next cooling or heating season without the negative effects of heat interference. Figure 7 shows the heat build-up that occurs when the half year BHE spacing occurs within the heat plume generated by adjacent BHEs. When such negative thermal interference occurs, it may be possible to space the BHEs at a distance that captures heat after a year and a half of transport instead of half a year of transport, which could be demonstrated in future simulations.

Simulations after ten years of operation

The long term effects of the optimized BHE spacing are investigated by simulating ten years of GSHP operation with four 90 day seasons per year: summer cooling at a constant heat transfer rate of 10 W/m into the ground, a fall no operation season, winter heating at a constant heat transfer rate of 10 W/m out of the ground, and a winter no operation season with one BHE (as seen in Figure 1). For these simulations, two groundwater flow velocities from the previous section (Section 2.3.2) are used: 5 x 10^{-5} m/s and 2.5 x 10^{-5} m/s as well as a no-groundwater-flow case.

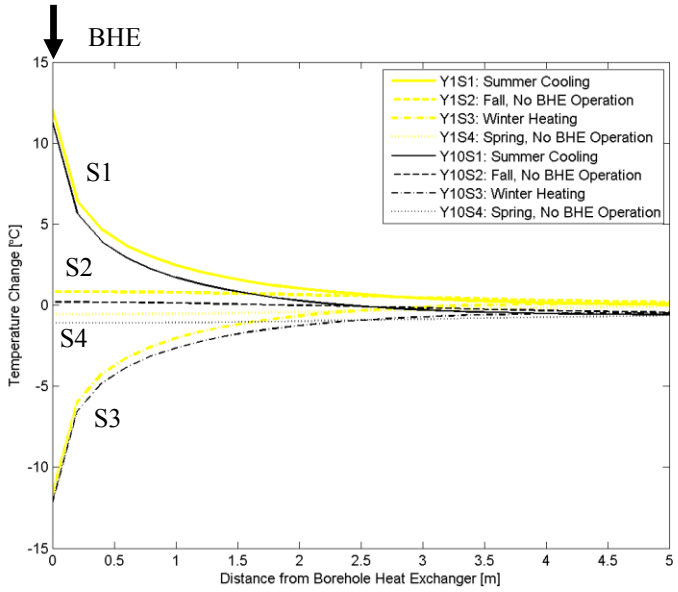

Figure 9. The temperature change in the aquifer surrounding a single BHE with a thermal diffusivity of 1.025 x 10^{-6} m^2/s and no groundwater flow velocity at the end of each season (90 days of summer cooling at a constant heat transfer rate of 10 W/m, 90 days of fall no BHE operation, 90 days of winter heating at a constant heat transfer rate of 10 W/m and 90 days of spring no BHE operation) for year 1 and 10 or a ten year simulation.

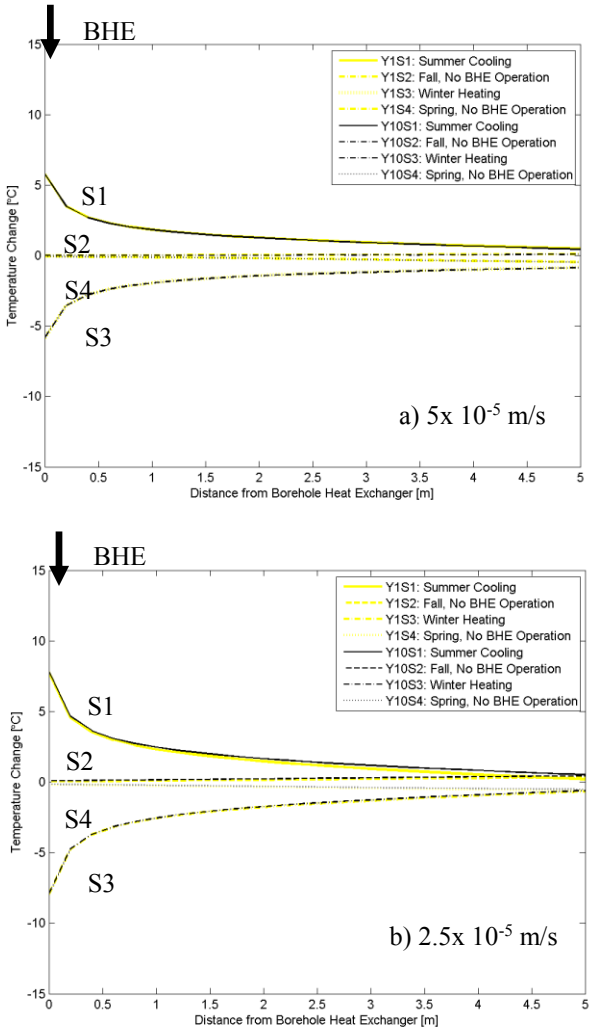

Figure 10. The temperature change in the aquifer surrounding a single BHE with a thermal diffusivity of 1.025 x 10^{-6} m^2/s and a groundwater flow velocity of a) 5 x 10^{-5} m/s and b) 2.5 x 10^{-5} m/s at the end of each season (90 days of summer cooling at a constant heat transfer rate of 10 W/m, 90 days of fall no BHE operation, 90 days of winter heating at a constant heat transfer rate of 10 W/m and 90 days of spring no BHE operation) for year 1 and 10 or a ten year simulation.

After ten years of operation, a difference in behavior becomes apparent between the cases with heat advection and the case without heat advection (the no groundwater flow case). In the case without heat advection, a steady state was not reached after ten years (see Figure 9) but was approached in the cases with heat advection (see Figure 10). Each year of operation, for the case without heat advection, results in a lowered background

temperature at the end of each season. At the start of the first year, the aquifer temperature equals the undisturbed temperature of the ground, but at the end of the first year, this temperature has been lowered by almost 0.5 °C (see Figure 9 and Figure 6d). So at the start of the next year, the BHE injects heat from summer cooling at a point in the aquifer that is lower in temperature than at the start of the previous year. This continues for each subsequent year in the ten-year simulation.

It is possible that this system could reach a steady state over time if the temperature shift is dampened with each year of operation. If this simulation was run starting with a winter heating system instead of a summer heating system, the cooling effect may be reversed. Each subsequent year would increase the background temperature of the aquifer, which may be more desirable in GSHP systems with higher heating loads or lower undisturbed ground temperatures.

The two cases with groundwater flow are dominated by heat advection with Péclet numbers of approximately 69 and 140. Thus, the heat near the BHE is carried away advectively by groundwater quickly enough to avoid interference with the heat exchanger during the following heating or cooling season. In GSHP systems with slower groundwater flow velocities, where heat advection is not as dominant, changes in the background temperatures similar to those seen in the no groundwater flow case are likely to occur.

3. Conclusions

For a ground source heat pump system (GSHP), there is a threshold groundwater flow velocity (that depends on the effective thermal diffusivity of the aquifer and on the ratio of heat advection rate to heat conduction rate as expressed by the Péclet number), beyond which heat transfer between the borehole heat exchangers (BHEs) and the aquifer is significantly increased, thus lowering the outlet temperature of the BHE necessary to input a constant amount of heat into the aquifer (lowering the temperature drop of the circulating fluid in the BHE) and increasing the overall efficiency of the GSHP system. The gain in heat transfer efficiency from groundwater heat advection is more pronounced in systems with lower thermal diffusivities and longer operational durations, though areas with higher thermal diffusivities and shorter operation times can still benefit from heat advection to a lesser extent. The simulations show that heat build-up near the heat exchanger is significantly reduced at a threshold groundwater flow velocity dependent on the given conditions. The threshold groundwater flow velocity is lower for systems with lower thermal diffusivities than for those with higher thermal diffusivities. This causes greater efficiency in system operation and potentially the reduction of in the number BHEs necessary, when considered during the design stages. The threshold Péclet number associated with a 1% change in BHE outlet temperature is approximately 2 and with a 5% change in BHE outlet temperature is approximately 11 for these simulations.

In GSHP systems using a standardized spacing between BHEs, groundwater heat advection can cause negative thermal interactions between BHEs. At higher groundwater flow velocities (more heat advection), longer operation times, and lower thermal diffusivities, heat may advect from one BHE to the next within a single operation season when aligned parallel to groundwater flow. Thus, the BHE outlet temperature at the downstream heat exchangers is increased, and overall system efficiency is decreased. By simulating the GSHP systems and choosing an optimum spacing between BHEs, these negative thermal interactions can be eliminated and in some situations replaced with positive thermal interactions.

For simulations with a thermal diffusivity of 1.025×10^{-6} m^2/s and a groundwater flow velocity less than 1×10^{-5} m/s (for the GSHP system parameters modeled), there is no spacing between heat exchangers that will allow for the utilization of the previous season's heat injection or extraction, a half year transport distance. The BHE placement in these systems should be determined based upon minimizing the negative thermal interactions between BHEs. It may be possible to space the BHEs, for systems with slight heat advection dominance, at a distance that captures heat after a year and a half of transport instead of half a year of transport. Multi-year simulations should be carried out to investigate the results of such a strategy.

At higher groundwater flow velocities (above 2.5×10^{-5} m/s for the GSHP system parameters modeled), BHE spacing for simulations with a thermal diffusivity of 1.025 x

10^{-6} m^2/s and heat advection dominance can be optimized to allow for the capture of temperature peaks and minimums for the next operation season and to reduce heat build-up or freezing in the GSHP system. The BHE spacings for optimization are 6.65 m and 13.8 m at groundwater flow velocities of 2.5 x 10^{-5} m/s and 5 x 10^{-5} m/s, respectively (for the GSHP system simulated in this study).

In GSHP systems with little heat advection, the background temperature of the aquifer changes with each year of operation during a ten-year simulation. This did not occur in systems with dominant heat advection. This system may reach a steady state over time if the temperature shift is dampened with each year of operation. In addition, the cooling effect may be reversed to a heating effect if the simulation was run starting with a winter heating season as opposed to a summer cooling season. Further simulations should be run to confirm these potential long-term behaviors.

References

2007 ASHRAE Handbook: Heating, Ventilating and Air-Conditioning Applications. 2007. American Society of Heating, Refrigerating and Air-Conditioning Engineers and Knovel (Firm), editors. Atlanta, Georgia: ASHRAE.

Banks, D. 2008. *An Introduction to Thermogeology: Ground Source Heating and Cooling.* Wiley-Blackwell, Oxford. Malden, MA.

Bobeck, P. 2004. *English Translation of Darcy (1856).* Kendall/Hunt. Dubuque, IA. 559p. ISBN 0-7575-0540-6.

Carslaw H.S. and J.C. Jaeger. 1959. *Conduction of Heat in Solids*. 2nd ed. Great Britain: Oxford University Press.

Chiasson A.D., S.J. Rees, and J.D. Spitler. 2000. A preliminary assessment of the effects of ground-water flow on closed-loop ground-source heat pump systems. *ASHRAE Transactions* 106(1):380-93.

Choi J.C., J. Park, and S.R. Lee. 2013. Numerical evaluation of the effects of groundwater flow on borehole heat exchanger arrays. *Renewable Energy* 52:230-40.

Clauser, C. 2003. *Numerical Simulation of Reactive Flow in Hot Aquifers*. Springer, Berlin.

Darcy H.P.G. 1856. *Les fountaines publiques de la Ville de Dijon* [The public fountains of the city of Dijon]. Dalmont, Paris.

De Vries, D. A. 1963. Thermal properties of soils. In: *Physics of Plant Environment*. W.R. van Wijk (ed). North-Holland, Amsterdam: 210-235.

Diao N., Q. Li, and Z. Fang. 2004. Heat transfer in ground heat exchangers with groundwater advection. *International Journal of Thermal Sciences* 43(12):1203-11.

Domenico P.A. and F.W. Schwartz. 1990. *Physical and Chemical Hydrogeology*. New York: Wiley.

Fan R., Y. Jiang, Y. Yao, D. Shiming, and Z. Ma. 2007. A study on the performance of a geothermal heat exchanger under coupled heat conduction and groundwater advection. *Energy* 32(11):2199-209.

Florides G.A., P. Christodoulides, and P. Pouloupatis. 2012. An analysis of heat flow through a borehole heat exchanger validated model. *Appl Energy* 92:523-33.

Fourier J.B.J. 1822. *Theorie Analytique de la Chaleur* [The analytical theory of heat]. Didot, Paris.

Freeze R.A. and J.A. Cherry. 1979. *Groundwater*. Englewood Cliffs, NJ: Prentice-Hall.

Fujii H., R. Itoi, J. Fujii, and Y. Uchida. 2005. Optimizing the design of large-scale ground-coupled heat pump systems using groundwater and heat transport modeling. *Geothermics* 34, 347–364.

Guo W. and C.D. Langevin. 2002. User's guide to SEAWAT: A computer program for simulation of three-dimensional variable-density ground-water flow. Tallahassee, Florida: U.S. Geological Survey. Report 6-A7.

Harbaugh A.W. 2005. MODFLOW-2005, the U.S. Geological Survey modular ground-water model -- the ground-water flow process. U.S. Geological Survey Techniques and Methods 6-A16.

Harbaugh A.W., E.R. Banta, M.C. Hill, and M.G. McDonald. 2000. MODFLOW-2000, the U.S. Geological Survey modular ground-water model, user guide to modularization concepts and the ground-water flow process. Reston, Virginia: U.S. Geological Survey Open-File Report 00-92.

Hecht-Méndez J., N. Molina-Giraldo, P. Blum, and P. Bayer. 2010. Evaluating MT3DMS for heat transport simulation of closed geothermal systems. *Ground Water* 48(5):741-56.

Ingersoll L.R. 1954. *Heat Conduction with Engineering, Geological, and Other Applications.* Madison: University of Wisconsin Press.

Koohi-Fayegh S. and M.A. Rosen. 2012. Examination of thermal interaction of multiple vertical ground heat exchangers. *Appl Energy* 97:962-9.

Langevin C.D., D.T. Thorne Jr., A.M. Dausman, M.C. Sukop, and W. Guo. 2008. *SEAWAT Version 4: A Computer Program for Simulation of Multi-Species Solute and Heat Transport. In: U.S. Geological Survey Techniques and Methods. Book 6,* Chapter A22. Reston, Virginia: USGS.

Lee C.K. 2011. Effects of multiple ground layers on thermal response test analysis and ground-source heat pump simulation. *Appl Energy* 88(12):4405-10.

Metzger T., S. Didierjean, and D. Maillet. 2004. Optimal experimental estimation of thermal dispersion coefficients in porous media. *International Journal of Heat and Mass Transfer* 47(14-16):3341-53.

Michopoulos A. and N. Kyriakis. 2009. Predicting the fluid temperature at the exit of the vertical ground heat exchangers. *Appl Energy* 86(10):2065-70.

Mottaghy D. and L. Dijkshoorn. 2012. Implementing an effective finite difference formulation for borehole heat exchangers into a heat and mass transport code. *Renewable Energy* 45:59-71.

Nakshabandi G.A. and H. Kohnke. 1965. Thermal conductivity and diffusivity of soils as related to moisture tension and other physical properties. *Agr Meteorol* 2:271-179.

Raymond J., R. Therrien, L. Gosselin L, and R. Lefebvre. 2011. Numerical analysis of thermal response tests with a groundwater flow and heat transfer model. *Renewable Energy* 36(1):315-24.

Saar, M. O., and M. Manga. 2004. Depth dependence of permeability in the Oregon Cascades inferred from hydrogeologic, thermal, seismic, and magmatic modeling constraints. *J. Geophys. Res.* 109. B04204, DOI 10.1029/2003JB002855.

Saar, M.O. 2011. Review: Geothermal heat as a tracer of large-scale groundwater flow and as a means to determine permeability fields, special theme issue on Environmental Tracers and Groundwater Flow, editor-invited peer-reviewed contribution, *Hydrogeology Journal* 19:31-52. DOI 10.1007/s10040-010-0657-2.

Sutton M., D. Nutter, and R. Couvillion. 2003. A ground resistance for vertical bore heat exchangers with groundwater flow. *Journal of Energy Resources Technology* 125(3):183-9.

Taler J and Duda P. 2006. *Solving Direct and Inverse Heat Conduction Problems*. The Netherlands: Springer.

U.S. Department of the Interior Geological Survey Water Resources Division. 1955. Redefinition of Coefficient of Storage. Washington, D.C. Memorandum No. 55.28. Code No. 45030.

VDI Heat Atlas. 2010. 2nd ed. Berlin; London: Springer.

Walsh, S.D.C. and M.O. Saar. 2010. Macroscale lattice-Boltzmann methods for low-Peclet-number solute and heat transport in heterogeneous porous media. *Water Resources Research* 46. W07517, DOI:10.1029/2009WR007895, 2010.

Wang H., Y. Cui, and C. Qi. 2013. Effects of sand-bentonite backfill materials on the thermal performance of borehole heat exchangers, *Heat Transfer Engineering* 34(1): 37-44.

Zheng C. 2009. Recent developments and future directions for MT3DMS and related transport codes. *Ground Water* 47(5):620-5.

Zheng C. 2010. *MT3DMS v5.3 Supplemental User's Guide*. Technical Report to the U.S. Army Engineer Research and Development Center.

Zheng C. and G.D. Bennett. 2002. *Applied Contaminant Transport Modeling*. 2nd ed. New York: John Wiley and Sons, Inc.

Zheng C., M.C. Hill, and P.A. Hsieh. 2001. MODFLOW-2000, the U.S. Geological Survey modular ground-water model, user guide to the LMT6 package, the linkage with MT3DMS for multi-species mass transport modeling. Denver, Colorado: U.S. Geological Survey Open File Report 01-82.

Zheng C. and P. Wang. 1999. MT3DMS: A modular three-dimensional multispecies transport model for simulation of advection, dispersion, and chemical reactions of contaminants in groundwater systems: Documentation and user's guide. U.S. Army Corps of Engineers; U.S. Army Engineer Research and Development Center Contract Report SERDP-99-1 Vicksburg, Mississippi, 221. http:/hydro.geo.ua.edu/mt3d/.

Appendix A: Model validation

As part of validating the groundwater heat transport models, MODFLOW and SEAWAT, the temperature distributions from conductive heat transport simulations are compared to the temperature distributions from an analytical solution for purely conductive heat transfer from a linear heat source with a constant heat exchange rate (Carslaw and Jaeger, 1959; Taler and Duda, 2006). This assumes an infinite, isotropic, and homogenous porous medium, a uniform initial temperature, and a constant temperature at an infinite radial distance from the source.

The temperature distribution for the analytic solution is calculated as follows:

$$\Delta T(r,t) = \frac{-q_i}{4\pi k_{eff}} E_i\left(\frac{-r^2}{4at}\right) \qquad (17)$$

where T is the temperature, q_i is the constant heat transfer per unit length of the borehole, k_{eff} is the effective thermal conductivity of the porous medium, $E_i()$ is the exponential integral, r is the radial distance from the BHE, a is the effective thermal diffusivity, and t is the time. Here, the exponential integral for real non-zero values of x is defined by:

$$E_i(x) = -\int_{-x}^{\infty} \frac{e^{-t}}{t} dt. \qquad (18)$$

The simulation and analytical solution results are compared for a summer cooling season of 100 days and a constant heat exchange rate of 60 W/m for a GSHP system with thermal properties listed in Table 8 and the same model configuration used for the single-BHE simulations previously described (Section 1.1). After 10 and 100 days of simulated

cooling, the temperature distributions from MT3DMS and SEAWAT are compared to the analytical solution using the method of efficiencies (Loagne and Green, 1991; Hecht-Méndez et al., 2010). The residual errors, or modeling efficiency, is calculated using the following:

$$EF=\frac{\sum_{i=1}^{n}(X_{(i)}-\bar{X})^2-\sum_{i=1}^{n}(X'_{(i)}-X_{(i)})^2}{\sum_{i=1}^{n}(X_{(i)}-\bar{X})^2} \qquad (19)$$

where EF is the modeling efficiency, $X_{(i)}$ are the 'observed/true' values, $\bar{X}$ is the mean of the 'observed/true' values, and $X'_{(i)}$ are the simulated values.

Table 8. BHE and aquifer properties used in model validation

Symbol	Property	Value	Units
q_i	Heat energy transfer per unit length of borehole	60	W/m
k_{eff}	Thermal conductivity, effective	2.0	W/m/K
n	Porosity	0.26	-
c_{ps}	Specific heat capacity, soil	880	J/kg/K
ρ_s	Density , soil	2650	kg/m^3
$\rho_w c_{pw}$	Volumetric heat capacity, water	4.186 x 10^{-6}	J/kg/K
α	Thermal diffusivity, effective	1.86 x 10^{-6}	m^2/s
t	Time	8.64 x 10^6	s

The modeling efficiency is 0.9247 for the MT3DMS simulation and 0.9248 for the SEAWAT simulation after 10 days of operation. The efficiency is somewhat increased after 100 days of operation with modeling efficiency of 0.9599 for both simulators. Thus, the analytical solution and simulation results are in good agreement. A visual comparison of the temperature distributions (Figure 11) also supports good agreement between model results and the analytical solution.

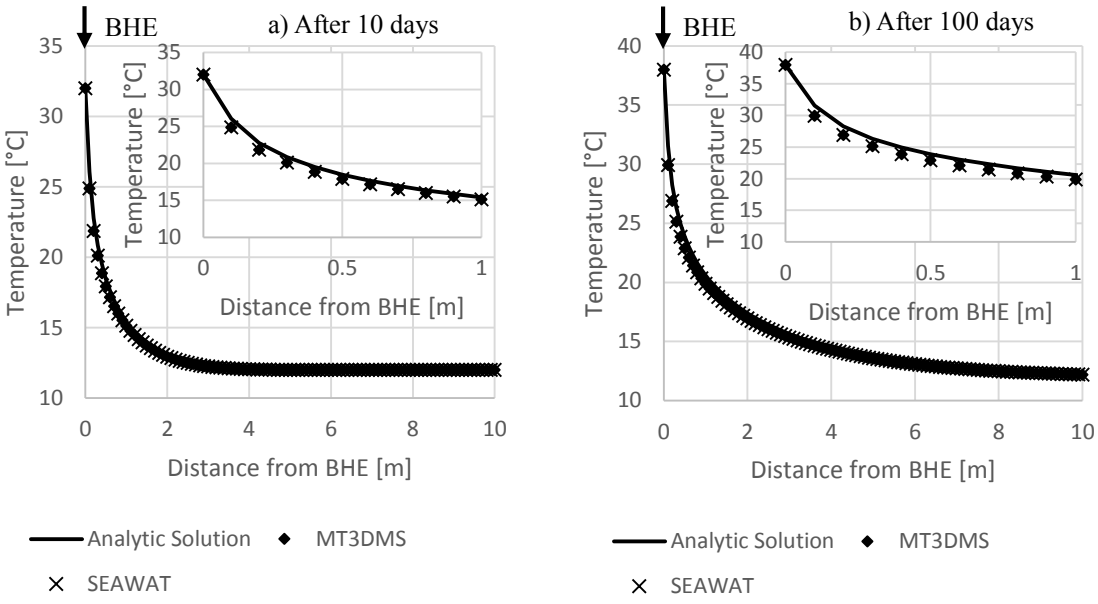

Figure 11. Comparison of analytic solution with temperature distributions resulting from MT3DMS and SEAWAT simulations of a) 10 days and b) 100 days of summer cooling at 60 W/m for a single BHE.

Appendix B: No thermal interference between BHE

Table 9. After 90 days of summer cooling at a constant heat exchange rate of 25 W/m from a single BHE into an aquifer with a thermal diffusivity of 1.025E-6 m^2/s.

Groundwater x-velocity [m/s]	Temperature at the BHE outlet [°C]	Temperature at the BHE wall [°C]	Percent change in BHE outlet temperature [%]	Percent change in BHE wall temperature [%]	Péclet number
0	39.4	42.3	0.00	0.00	0.00
5E-9	39.4	42.2	0.08	0.07	0.01
1E-8	39.4	42.2	0.08	0.07	0.03
5E-8	39.4	42.2	0.15	0.14	0.14
1E-7	39.4	42.2	0.20	0.19	0.28
5E-7	39.2	42.0	0.68	0.64	1.38
1E-6	38.9	41.7	1.32	1.23	2.77
5E-6	37.0	39.8	6.24	5.82	13.84
1E-5	34.7	37.5	11.99	11.19	27.68
2.5E-5	29.3	32.1	25.66	23.95	69.21

Table 10. After 30 days of summer cooling at a constant heat exchange rate of 25 W/m from a single BHE into an aquifer with a thermal diffusivity of 1.025E-6 m^2/s.

Groundwater x-velocity [m/s]	Temperature at the BHE outlet [°C]	Temperature at the BHE wall [°C]	Percent change in BHE outlet temperature [%]	Percent change in BHE wall temperature [%]	Péclet number
0	36.0	38.9	0.00	0.00	0.00
5E-9	36.0	38.9	0.00	0.00	0.01
1E-8	36.0	38.8	0.03	0.03	0.03
5E-8	36.0	38.8	0.08	0.07	0.14
1E-7	36.0	38.8	0.14	0.13	0.28
5E-7	35.8	38.6	0.61	0.57	1.38
1E-6	35.9	38.4	1.19	1.11	2.77
5E-6	34.0	36.8	5.64	5.23	13.84
1E-5	32.2	35.1	10.52	9.76	27.68
2.5E-5	28.1	31.0	21.90	20.31	69.21

Table 11. After 180 days of summer cooling at a constant heat exchange rate of 25 W/m from a single BHE into an aquifer with a thermal diffusivity of 1.025E-6 m^2/s.

Groundwater x-velocity [m/s]	Temperature at the BHE outlet [°C]	Temperature at the BHE wall [°C]	Percent change in BHE outlet temperature [%]	Percent change in BHE wall temperature [%]	Péclet number
0	41.5	44.4	0.00	0.00	0.00
5E-9	41.5	44.4	0.02	0.02	0.01
1E-8	41.5	44.4	0.02	0.02	0.03
5E-8	41.5	44.3	0.07	0.07	0.14
1E-7	41.5	43.3	0.12	0.11	0.28
5E-7	41.3	44.1	0.65	0.61	1.38
1E-6	41.0	43.8	1.30	1.22	2.77
5E-6	38.7	41.6	6.79	6.36	13.85
1E-5	35.9	38.8	13.48	12.62	27.69
2.5E-5	29.5	32.4	28.89	27.05	69.23

Table 12. After 90 days of summer cooling at a constant heat exchange rate of 25 W/m from a single BHE into an aquifer with a thermal diffusivity of 1.507E-6 m^2/s.

Groundwater x-velocity [m/s]	Temperature at the BHE outlet [°C]	Temperature at the BHE wall [°C]	Percent change in BHE outlet temperature [%]	Percent change in BHE wall temperature [%]	Péclet number
0	30.5	33.4	0.00	0.00	0.00
5E-9	30.5	33.4	-0.03	-0.03	0.01
1E-8	30.5	33.4	-0.03	-0.03	0.02
5E-8	30.5	33.4	-0.03	-0.03	0.09
1E-7	30.5	33.4	0.03	0.03	0.19
5E-7	30.4	33.3	0.36	0.33	0.94
1E-6	30.3	33.1	0.75	0.69	1.88
5E-6	29.3	32.2	3.93	3.60	9.42
1E-5	28.1	31.0	7.86	7.19	18.84
2.5E-5	24.9	27.8	18.37	16.82	47.09

Table 13. After 90 days of summer cooling at a constant heat exchange rate of 25 W/m from a single BHE into an aquifer with a thermal diffusivity of 5.431E-7 m^2/s.

Groundwater x-velocity [m/s]	**Temperature at the BHE outlet [°C]**	**Temperature at the BHE wall [°C]**	**Percent change in BHE outlet temperature [%]**	**Percent change in BHE wall temperature [%]**	**Péclet number**
0	62.5	65.4	0.00	0.00	0.00
5E-9	62.5	65.4	0.02	0.02	0.03
1E-8	62.5	65.4	0.03	0.03	0.05
5E-8	62.5	65.3	0.14	0.14	0.26
1E-7	62.4	65.2	0.26	0.24	0.52
5E-7	61.7	64.6	1.31	1.25	2.61
1E-6	60.9	63.8	2.57	2.46	5.23
5E-6	55.2	58.0	11.82	11.30	26.13
1E-5	49.3	52.1	21.22	20.30	52.27
2.5E-5	37.9	40.7	39.41	37.71	130.67

Appendix C: Thermal interference between BHEs

Table 14. After 90 days of summer cooling at a constant heat exchange rate of 25 W/m from three BHEs positioned parallel to groundwater flow into an aquifer with a thermal diffusivity of 1.025E-6 m^2/s.

Groundwater x-velocity [m/s]	Temperature at the BHE outlet [°C]			Temperature at the BHE wall [°C]		
	BHE 1	**BHE 2**	**BHE 3**	**BHE1**	**BHE 2**	**BHE 3**
0	39.6	39.7	39.6	42.4	42.6	42.4
5E-9	39.6	39.7	39.5	42.4	42.5	42.4
1E-8	39.5	39.7	39.5	42.4	42.5	42.4
5E-8	39.5	39.7	39.5	42.4	42.5	42.4
1E-7	39.5	39.7	39.5	42.3	42.5	42.3
5E-7	39.3	39.5	39.3	42.1	42.3	42.2
1E-6	39.0	39.2	39.1	41.9	42.1	41.9
5E-6	37.1	37.4	37.4	39.9	40.3	40.2
1E-5	34.8	35.5	35.4	37.6	38.3	38.3
2.5E-5	29.3	31.1	31.2	32.2	33.9	34.1

Groundwater x-velocity [m/s]	Percent change in BHE outlet temperature [%]			Percent change in BHE wall temperature [%]			Péclet number
	BHE 1	**BHE 2**	**BHE 3**	**BHE 1**	**BHE 2**	**BHE 3**	
0	0.00	0.00	0.00	0.00	0.00	0.00	0.00
5E-9	0.08	0.10	0.10	0.07	0.09	0.09	0.01
1E-8	0.10	0.13	0.10	0.09	0.12	0.09	0.03
5E-8	0.15	0.15	0.15	0.14	0.14	0.14	0.14
1E-7	0.20	0.20	0.20	0.19	0.19	0.19	0.28
5E-7	0.71	0.65	0.66	0.66	0.61	0.61	1.38
1E-6	1.36	1.26	1.24	1.27	1.17	1.55	2.77
5E-6	6.37	5.76	5.63	5.94	5.38	5.26	13.84
1E-5	12.15	10.67	10.48	11.34	9.96	9.79	27.68
2.5E-5	25.89	21.77	21.12	24.17	20.32	19.71	69.21

Table 15. After 30 days of summer cooling at a constant heat exchange rate of 25 W/m from three BHEs positioned parallel to groundwater flow into an aquifer with a thermal diffusivity of 1.025E-6 m^2/s.

Groundwater x-velocity [m/s]	Temperature at the BHE outlet [°C]			Temperature at the BHE wall [°C]		
	BHE 1	**BHE 2**	**BHE 3**	**BHE1**	**BHE 2**	**BHE 3**
0	36.0	36.0	36.0	38.9	38.9	38.9
5E-9	36.0	36.0	36.0	38.9	38.9	38.8
1E-8	36.0	36.0	36.0	38.8	38.8	38.8
5E-8	36.0	36.0	36.0	38.8	38.8	38.8
1E-7	36.0	36.0	36.0	38.8	38.8	38.8
5E-7	35.8	35.8	35.8	38.6	38.6	38.6
1E-6	35.6	35.6	35.6	38.4	38.4	38.4
5E-6	34.0	34.0	34.0	36.8	36.8	36.8
1E-5	32.2	32.3	32.3	35.1	35.1	35.1
2.5E-5	28.1	28.3	28.3	31.0	31.1	31.1

Groundwater x-velocity [m/s]	Percent change in BHE outlet temperature [%]			Percent change in BHE wall temperature [%]			Péclet number
	BHE 1	**BHE 2**	**BHE 3**	**BHE 1**	**BHE 2**	**BHE 3**	
0	0.00	0.00	0.00	0.00	0.00	0.00	0.00
5E-9	0.00	0.00	0.03	0.00	0.00	0.03	0.01
1E-8	0.03	0.03	0.03	0.03	0.03	0.03	0.03
5E-8	0.08	0.06	0.06	0.08	0.05	0.05	0.14
1E-7	0.14	0.11	0.11	0.13	0.10	0.10	0.28
5E-7	0.61	0.61	0.61	0.57	0.57	0.57	1.38
1E-6	1.19	1.19	1.19	1.11	1.11	1.11	2.77
5E-6	5.64	5.61	5.61	5.23	5.20	5.20	13.84
1E-5	10.52	10.47	10.47	9.76	9.70	9.70	27.68
2.5E-5	21.90	21.54	21.54	20.31	19.97	19.97	69.21

Table 16. After 180 days of summer cooling at a constant heat exchange rate of 25 W/m from three BHEs positioned parallel to groundwater flow into an aquifer with a thermal diffusivity of 1.025E-6 m^2/s.

Groundwater x-velocity [m/s]	Temperature at the BHE outlet [°C]			Temperature at the BHE wall [°C]		
	BHE 1	**BHE 2**	**BHE 3**	**BHE1**	**BHE 2**	**BHE 3**
0	42.2	42.9	42.2	45.0	45.7	45.0
5E-9	42.2	42.9	42.2	45.0	45.7	45.0
1E-8	42.2	42.9	42.2	45.0	45.7	45.0
5E-8	42.2	42.8	42.2	45.0	45.7	45.0
1E-7	42.2	42.8	42.2	45.0	45.7	45.0
5E-7	41.9	42.6	42.0	44.7	45.5	44.9
1E-6	41.6	42.4	41.8	44.4	45.2	44.7
5E-6	39.1	40.5	40.2	41.9	43.3	43.1
1E-5	36.1	38.3	38.4	39.0	41.2	41.2
2.5E-5	29.6	32.6	33.8	32.4	35.4	36.7

Groundwater x-velocity [m/s]	Percent change in BHE outlet temperature [%]			Percent change in BHE wall temperature [%]			Péclet number
	BHE 1	**BHE 2**	**BHE 3**	**BHE 1**	**BHE 2**	**BHE 3**	
0	0.00	0.00	0.00	0.00	0.00	0.00	0.00
5E-9	0.00	0.00	0.02	0.00	0.00	0.02	0.01
1E-8	0.02	0.02	0.02	0.02	0.22	0.02	0.03
5E-8	0.07	0.05	0.05	0.07	0.04	0.04	0.14
1E-7	0.14	0.09	0.07	0.13	0.09	0.07	0.28
5E-7	0.73	0.56	0.45	0.69	0.53	0.42	1.38
1E-6	1.47	1.10	0.92	1.38	1.03	0.87	2.77
5E-6	7.41	5.48	4.71	6.95	5.14	4.42	13.84
1E-5	14.38	10.66	9.05	13.48	9.91	8.48	27.68
2.5E-5	29.92	23.94	19.83	28.04	22.46	18.58	69.21

Table 17. After 90 days of summer cooling at a constant heat exchange rate of 25 W/m from three BHEs positioned parallel to groundwater flow into an aquifer with a thermal diffusivity of 5.431E-7 m^2/s.

Groundwater x-velocity [m/s]	Temperature at the BHE outlet [°C]			Temperature at the BHE wall [°C]		
	BHE 1	**BHE 2**	**BHE 3**	**BHE1**	**BHE 2**	**BHE 3**
0	62.6	62.6	62.6	65.4	65.4	65.4
5E-9	62.6	62.6	62.6	65.4	65.4	65.4
1E-8	62.6	62.6	62.6	65.4	65.4	65.4
5E-8	62.5	62.5	62.5	65.3	65.3	65.3
1E-7	62.4	62.4	62.4	65.2	65.3	65.2
5E-7	61.8	61.8	61.8	64.6	64.6	64.6
1E-6	61.0	61.0	61.0	63.8	63.8	63.8
5E-6	55.2	55.4	55.4	58.0	58.2	58.2
1E-5	49.3	49.9	49.9	52.1	52.8	52.8
2.5E-5	37.9	40.3	40.4	40.7	43.1	43.3

Groundwater x-velocity [m/s]	Percent change in BHE outlet temperature [%]			Percent change in BHE wall temperature [%]			Péclet number
	BHE 1	**BHE 2**	**BHE 3**	**BHE 1**	**BHE 2**	**BHE 3**	
0	0.00	0.00	0.00	0.00	0.00	0.00	0.00
5E-9	0.02	0.00	0.02	0.02	0.00	0.02	0.03
1E-8	0.03	0.02	0.03	0.03	0.02	0.03	0.05
5E-8	0.13	0.13	0.13	0.14	0.12	0.12	0.26
1E-7	0.27	0.26	0.27	0.26	0.24	0.26	0.52
5E-7	1.31	1.28	1.29	1.25	1.22	1.24	2.61
1E-6	2.57	2.54	2.54	2.46	2.43	2.43	5.23
5E-6	11.83	11.50	11.52	11.32	11.01	11.02	23.13
1E-5	21.24	20.21	20.20	20.32	19.34	19.33	52.25
2.5E-5	39.44	35.63	35.40	37.74	34.09	33.87	130.63

Table 18. After 90 days of summer cooling at a constant heat exchange rate of 25 W/m from three BHEs positioned parallel to groundwater flow into an aquifer with a thermal diffusivity of 1.507E-6 m^2/s.

Groundwater x-velocity [m/s]	Temperature at the BHE outlet [°C]			Temperature at the BHE wall [°C]		
	BHE 1	**BHE 2**	**BHE 3**	**BHE1**	**BHE 2**	**BHE 3**
0	30.8	31.0	30.8	33.6	33.9	33.6
5E-9	30.9	31.1	30.8	33.6	33.9	33.6
1E-8	30.8	31.1	30.8	33.6	33.9	33.6
5E-8	30.8	31.1	30.8	33.6	33.9	33.6
1E-7	30.8	31.0	30.8	33.6	33.9	33.6
5E-7	30.7	30.9	30.7	33.5	33.8	33.5
1E-6	30.5	30.8	30.6	33.4	33.7	33.4
5E-6	29.5	30.0	29.8	32.3	32.8	32.6
1E-5	28.3	29.0	28.9	31.1	31.8	31.7
2.5E-5	25.0	26.4	26.5	27.8	29.2	29.4

Groundwater x-velocity [m/s]	Percent change in BHE outlet temperature [%]			Percent change in BHE wall temperature [%]			Péclet number
	BHE 1	**BHE 2**	**BHE 3**	**BHE 1**	**BHE 2**	**BHE 3**	
0	0.00	0.00	0.00	0.00	0.00	0.00	0.00
5E-9	-0.07	-0.06	-0.07	-0.06	-0.06	-0.06	0.01
1E-8	-0.07	-0.06	-0.07	-0.06	-0.06	-0.06	0.02
5E-8	-0.07	-0.06	-0.07	-0.06	-0.06	-0.06	0.09
1E-7	0.03	0.03	0.03	0.03	0.03	0.03	0.19
5E-7	0.39	0.32	0.29	0.36	0.30	0.27	0.95
1E-6	0.81	0.68	0.62	0.74	0.62	0.57	1.89
5E-6	4.16	3.45	3.15	3.81	3.16	2.89	9.46
1E-5	8.22	6.61	6.17	7.53	6.05	5.65	18.91
2.5E-5	18.91	14.92	13.77	17.32	13.67	12.62	47.29

Appendix D: Optimization of BHE spacing

Table 19. After 90 days of summer cooling at a constant heat exchange rate of 10 W/m from a single BHE into an aquifer with a thermal diffusivity of 1.025E-6 m^2/s.

Groundwater x-velocity [m/s]	Temperature at the BHE outlet [°C]	Temperature at the BHE wall [°C]	Percent change in BHE outlet temperature [%]	Percent change in BHE wall temperature [%]	Péclet number
0	21.3	24.1	0.00	0.00	0.00
5E-9	21.3	24.1	0.14	0.12	0.01
1E-8	21.3	24.1	0.14	0.12	0.03
5E-8	21.2	24.1	0.19	0.17	0.14
1E-7	21.2	24.1	0.19	0.17	0.28
5E-7	21.1	24.0	0.56	0.50	1.38
1E-6	21.1	23.9	1.03	0.91	2.77
5E-6	20.3	23.1	4.70	4.15	13.84
1E-5	19.4	22.2	8.93	7.88	27.68
2.5E-5	17.2	20.0	19.12	16.88	69.21
5E-5	15.1	17.9	29.04	25.63	138.41
7.5E-5	13.9	16.7	34.77	30.69	207.62
1E-4	13.1	16.0	38.34	33.84	276.82

Table 20. After 90 days of summer cooling at a constant heat exchange rate of 10 W/m and 90 days of fall no BHE operation from a single BHE into an aquifer with a thermal diffusivity of 1.025E-6 m^2/s.

Groundwater x-velocity [m/s]	Temperature at the BHE wall [°C]	Percent change in BHE wall temperature [%]	Péclet number	Max temperature change[°C]	Distance from 1st BHE [m]
0	12.9	0.00	0.00	0.88	0.0
5E-9	12.9	0.23	0.01	0.85	0.0
1E-8	12.8	0.31	0.03	0.84	0.0
5E-8	12.8	0.31	0.14	0.84	0.0
1E-7	12.9	0.23	0.28	0.85	0.0
5E-7	12.8	0.31	1.38	0.84	0.0
1E-6	12.8	0.39	2.77	0.83	0.0
5E-6	12.7	1.40	13.84	0.77	1.2/1.4
1E-5	12.5	2.95	27.68	0.71	2.8
2.5E-5	12.1	6.06	69.21	0.53	6.8/7
5E-5	12.0	6.83	138.41	0.44	13.8
7.5E-5	12.0	7.07	207.62	0.29	20.6/20.8
1E-4	12.0	6.91	276.82	0.21	27.4

Table 21. After 90 days of summer cooling at a constant heat exchange rate of 10 W/m, 90 days of fall no BHE operation, and 90 days of winter heating at a constant heat exchange rate of 10 W/m between a single BHE and of an aquifer with a thermal diffusivity of 1.025E-6 m^2/s.

Groundwater x-velocity [m/s]	Temperature at the BHE outlet [°C]	Temperature at the BHE wall [°C]	Percent change in BHE outlet temperature [%]	Percent change in BHE wall temperature [%]	Péclet number
0	-2.4	0.4	0.00	0.00	0.00
5E-9	-2.4	0.4	-1.24	7.14	0.01
1E-8	-2.4	0.4	-1.25	7.14	0.03
5E-8	-2.4	0.4	-0.83	4.76	0.14
1E-7	-2.4	0.4	-0.42	2.38	0.28
5E-7	-2.3	0.5	2.49	-14.29	1.38
1E-6	-2.2	0.6	6.65	-38.10	2.77
5E-6	-1.6	1.3	34.49	-197.62	13.84
1E-5	-0.8	2.0	65.66	-376.19	27.68
2.5E-5	1.1	3.9	146.28	-838.10	69.21
5E-5	3.2	6.1	233.97	-1340.48	138.41
7.5E-5	4.4	7.2	283.00	-1621.43	207.62
1E-4	5.2	8.0	316.25	-1811.90	276.82

**Note: The negative temperatures at the BHE outlet indicate that heating could not be accomplished for the entire simulated season. In real situations, the BHE would freeze up and further heat extraction from the aquifer would not be possible. At velocities of 1E-5 m/s and below (for an aquifer with this thermal diffusivity and other characteristics), heating at this level would only be possible for part of the season or intermittently over the course of the whole season. Also, it should be noted that due to the freezing of the BHE at lower velocities the percent change in BHE wall temperature is a better measure than the percent change in BHE outlet temperature.*

Table 22. After 90 days of summer cooling at a constant heat exchange rate of 10 W/m, 90 days of fall no BHE operation, 90 days of winter heating at a constant heat exchange rate of 10 W/m, and 90 days of spring no BHE operation between a single BHE and an aquifer with a thermal diffusivity of 1.025E-6 m^2/s.

Groundwater x-velocity [m/s]	**Temperature at the BHE wall [°C]**	**Percent change in BHE wall temperature [%]**	**Péclet number**
0	11.5	0.00	0.00
5E-9	11.5	0.26	0.01
1E-8	11.5	0.26	0.03
5E-8	11.5	0.26	0.14
1E-7	11.5	0.17	0.28
5E-7	11.5	0.17	1.38
1E-6	11.5	0.17	2.77
5E-6	11.5	-0.17	13.84
1E-5	11.6	-0.78	27.68
2.5E-5	11.9	-2.95	69.21
5E-5	12.0	-4.08	138.41
7.5E-5	12.0	-4.13	207.62
1E-4	12.0	-4.17	276.82

Groundwater x-velocity [m/s]	**Max temperature change[°C]**	**Distance from 1st BHE [m]**	**Min temperature change[°C]**	**Distance from 1st BHE [m]**
0	**0.07**	**7.4**	**-0.49**	**0**
5E-9	**0.04**	7	-0.52	0
1E-8	**0.03**	6.6	-0.52	0
5E-8	**0.04**	6.6	-0.52	0
1E-7	**0.04**	6.4	-0.51	0
5E-7	**0.05**	6.8	-0.51	0
1E-6	**0.06**	7	-0.51	0
5E-6	**0.1**	8.2	-0.51	1
1E-5	**0.16**	10.8	-0.52	2.2
2.5E-5	**0.18**	18.6	-0.55	6.4
5E-5	**0.22**	34.8	-0.38	13.8